

UCSF

UC San Francisco Electronic Theses and Dissertations

Title

Interleukin 6 is increased in preclinical HNSCC models of acquired cetuximab resistance, but is not required for maintenance of resistance

Permalink

<https://escholarship.org/uc/item/59j6p2c4>

Author

O'Keefe, Rachel

Publication Date

2019

Supplemental Material

<https://escholarship.org/uc/item/59j6p2c4#supplemental>

Peer reviewed|Thesis/dissertation

Interleukin 6 is increased in preclinical HNSCC models of acquired cetuximab resistance, but is not required for maintenance of resistance

by
Rachel O'Keefe

DISSERTATION

Submitted in partial satisfaction of the requirements for degree of
DOCTOR OF PHILOSOPHY

in

Biomedical Sciences

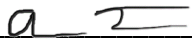
in the

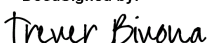
GRADUATE DIVISION

of the

UNIVERSITY OF CALIFORNIA, SAN FRANCISCO

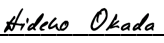
Approved:

DocuSigned by:

7D7A13DE0D5746E... Aaron Tward
Chair

DocuSigned by:

4F46D... Trever Bivona

DocuSigned by:

4FE... Jennifer Grandis

DocuSigned by:

17A559E4340249B... Hideho Okada

Committee Members

Acknowledgments

Thank you to my PI Jennifer Grandis, Dan Johnson, and Patrick Ha, who co-lead the Head and Neck Signaling Laboratory, and to all past and current members of the lab. I appreciate what I've learned from each of you and wish you all the best. I would especially like to thank Neil Bhola for his mentorship and dedication to the lab, and for our many discussions about science. To Janice Cho and Rodell Santuray: I am inspired by your commitment to using your many talents to make the world a better, healthier place, and your continuing friendship means the world to me. I would also like to thank our collaborators, especially Danielle Swaney, Margaret Soucheray, and Mehdi Bouhaddou, for sharing their expertise and for being excellent colleagues.

Thank you to every PI who has given me the opportunity to work in their lab and to the many colleagues who have provided guidance and friendship along the way. I would especially like to thank Angelique Bordey, Chris Bartley, Martin McMahon, and the members of the Bordey and McMahon labs. To Angelique: Thank you for fostering a supportive lab environment characterized by frequent discussions about science – working in your lab showed me how much fun science could be – and for your continued support. To Chris: I can't thank you enough for your mentorship and guidance during my three years in the Bordey lab. Thank you for teaching me important skills, like how to run a western blot and how to critically read a paper, and perhaps most importantly, for demonstrating by example how to persevere and follow the data when results don't align with expectations. To Martin: Though I only worked in your lab for a year, it would not be an exaggeration to say that I use what I learned from you every time I design an experiment. Thank you for sharing your vast scientific knowledge and for taking every opportunity to uphold the highest standards of science.

Thank you to the members of my thesis committee: Aaron Tward, Hideho Okada, and Trever Bivona. Your questions and comments have shaped the way I think about science, and I look forward to applying what you've taught me in the next lab I work in. While I greatly value your scientific expertise, what has perhaps meant even more is your support and advice when grad school became the most difficult. Thank you.

So much goes on behind the scenes to make research and training possible. To Demian Sainz, Lisa Magargal, Monique Piazza, Ned Molyneaux, and the many others who have worked in the BMS Administrative Office in the past six years: Thank you for all you've done, from welcoming our group during the second BMS interview weekend in 2013 to guiding me through submitting this dissertation and graduating. I am in awe of your ability to wrangle dozens of grad students with different interests and goals and have always enjoyed chatting with you all at BMS events – thank you for having my back throughout the years. Thank you, also, to the past and current team in the UCSF Otolaryngology – Head & Neck Surgery department, especially Idonnah Hipolito, Joanna Times, and Scarlett Jin, who have gone above and beyond to help secure and distribute funding.

Every day, I am grateful for the support of friends near and far. There are a few people, in particular, whose friendship has made finishing grad school possible. To Gen Tsoi and James Lee: I've lost count of how many "talking points" we've discussed in 10+ years of friendship, but I do know just how lucky I am to have you guys in my life! I look forward to seeing you much more frequently now that I'll be living back on the East Coast. To Adrienne Stormo, Annalise Petriello, Dan Holohan, Drew McKinney, Jillian Jespersen, KT Nguyen, Lindsey Jones, Onur Erbilgin, Pallavi Penumetcha, and Thomas Hennings: Some of my favorite memories (not just from grad school, but ever!) are from the times we've laughed through trivia

nights, themed movie nights, and game nights (and the times we've hung out during the day, too). Without question, what I value most about my time in San Francisco is having had the opportunity to meet you all. Thank you for everything.

Thank you, most of all, to my family.

To my cousins Avery, Joseph, Julia, Kiley, Lucy, and Margaret: Spending time with you all on family vacations was the best possible break from lab! Thank you for sharing your adventures and achievements with us as you grow up.

To Aunt Lisa: Growing up, I always looked up to you as the cool aunt...and still do. Thank you for letting us hang out with you even when you were a teenager, and for inspiring me to take risks.

To Grandmom: From my earliest memories of looking at "Mr. Moon" and sitting on the couch and talking with you and Grandpop, to our cross-country phone calls and time spent together at the beach more recently, your love and support have been a constant. Thank you, for everything. I'm so happy we'll be living closer to each other soon! Bob, you've been a wonderful addition to our family, and I appreciate your support as well!

To my sister, Meg: Your network of friends since childhood is a testament to what a kind, clever, generous, fun person you are, and I'm so lucky that you're my sister. Thank you for making me laugh, listening to me cry, and for visiting San Francisco/letting me visit you in Chicago!

To my brother, John: I can always count on my favorite brother for a laugh and a spirited discussion when we talk on the phone – I always appreciate your intelligent perspectives, even when we disagree! Thank you, especially, for keeping me grounded, for laughing at my jokes (even if you deny that you laughed!), and for introducing our family to Jackbox games.

To my parents, Fran and John: I can't put into words how much your unwavering love and support means to me. I wouldn't be here without your providing so many opportunities to learn and grow and instilling the value of education in us. Through it all, I can't think of a moment when you've doubted what I could achieve, and even though I know you're biased, your belief and pride in me drive me to do better, always. Thank you for your constant encouragement in the past six years, and, not least, for making me laugh during the lows. I could keep going, but as I'm sure you can guess, I'm crying as I write this, and people walking by probably think something is wrong. I will say the rest in person, but for now: Thank you, and I love you.

Contributions

Chapter 1

Portions of this chapter were adapted from a manuscript (“Interleukin 6 is increased in preclinical HNSCC models of acquired cetuximab resistance, but is not required for maintenance of resistance”) by Rachel A. O’Keefe, Neil E. Bhola, David S. Lee, Daniel E. Johnson, and Jennifer R. Grandis that is currently in review at *PLOS ONE*. One section of this chapter was previously published in a chapter (“Targeting Members of the Epidermal Growth Factor Receptor Family to Improve Response to Chemotherapy,” in *Targeting Cell Survival Pathways to Enhance Response to Chemotherapy*) co-authored by Jennifer Grandis and Daniel Johnson. Sections of this chapter were previously published in a review article (“Targeting the IL-6/JAK/STAT3 signalling axis in cancer”) in *Nature Reviews Clinical Oncology* co-authored by Daniel Johnson and Jennifer Grandis. I wrote the text, and input was provided by all co-authors listed.

Chapter 2

This chapter contains text, figures, and a table from the aforementioned manuscript, and one section of the chapter was previously published in the aforementioned review article. Neil Bhola generated the cetuximab-resistant PE/CA-PJ49 cells used in this study and provided scientific input and guidance throughout the project. David Lee performed independent replication of several experiments in the study. Jennifer Grandis and Daniel Johnson provided input and guidance throughout the project. I wrote the text, designed and performed experiments, and performed statistical analyses, with input provided by all co-authors listed. The members of my

thesis committee (Trever Bivona, Hideho Okada, and Aaron Tward) provided helpful guidance throughout the project.

Chapter 3

Sections of this chapter, including Tables 3.1 and 3.2, are included in the aforementioned manuscript. Neil Bholra generated the cetuximab-resistant PE/CA-PJ49 cells analyzed. Jennifer Grandis and Daniel Johnson provided input on interpretation of data. I extracted genomic DNA for sequencing analysis, performed data analysis and generated tables, and wrote the text, with input from all co-authors listed. The UCSF Clinical Cancer Genomics Laboratory (CCGL) performed the UCSF500 sequencing, and Jessica Van Ziffle at the CCGL provided guidance on data analysis and presentation. Trever Bivona, Hideho Okada, and Aaron Tward suggested performing this analysis and provided input on interpretation of the results.

Chapter 4

Text from this chapter and Table 4.1 are included in the aforementioned manuscript. I wrote the text, and input was provided by all co-authors listed. The UCSF500 section was written with help from Jessica Van Ziffle.

**Interleukin 6 is increased in preclinical HNSCC models of acquired cetuximab resistance,
but is not required for maintenance of resistance**

Rachel Alexandra O'Keefe

Abstract

The epidermal growth factor receptor inhibitor cetuximab is the only oncogene-targeted agent that has been FDA approved for the treatment of head and neck squamous cell carcinoma (HNSCC). Currently, there are no biomarkers used in the clinic to predict which HNSCC tumors will respond to cetuximab, and even in tumors that regress with treatment, acquired resistance occurs in the majority of cases. Though a number of mechanisms of acquired resistance to cetuximab have been identified in preclinical studies, no therapies targeting these resistance pathways have yet been effectively translated into the clinic. To address this unmet need, we examined the role of the cytokine interleukin 6 (IL-6) in acquired cetuximab resistance in preclinical models of HNSCC. We found that IL-6 secretion was increased in PE/CA-PJ49 cells that had acquired resistance to cetuximab compared to the parental cells from which they were derived. However, addition of exogenous IL-6 to parental cells did not promote cetuximab resistance, and inhibition of the IL-6 pathway did not restore cetuximab sensitivity in the cetuximab-resistant cells. Further examination of the IL-6 pathway revealed that expression of *IL6R*, which encodes a component of the IL-6 receptor, was decreased in cetuximab-resistant cells compared to parental cells, and that treatment of the cetuximab-resistant cells with exogenous IL-6 did not induce phosphorylation of signal transducer and activator of transcription 3, suggesting that the IL-6 pathway was functionally impaired in the cetuximab-resistant cells. These findings demonstrate that, even if IL-6 is increased in the context of cetuximab resistance,

it is not necessarily required for maintenance of the resistant phenotype, and that targeting the IL-6 pathway may not restore sensitivity to cetuximab in cetuximab-refractory HNSCC.

Table of Contents

Chapter 1: Introduction.....	1
1.1 HNSCC incidence and etiology.....	1
1.2 Current treatment strategies in HNSCC.....	2
1.3 EGFR signaling and alterations in cancer.....	2
1.4 Cetuximab: An EGFR-targeted therapy used to treat HNSCC.....	4
1.5 Challenges in using cetuximab to treat HNSCC.....	5
Chapter 2: Interleukin 6 is increased in preclinical HNSCC models of acquired cetuximab resistance, but is not required for maintenance of resistance.....	9
2.1 Introduction.....	9
2.2 Results.....	14
2.3 Discussion.....	21
2.4 Figures.....	27
Chapter 3: Targeted sequencing analysis of cetuximab-sensitive and cetuximab- resistant variants of an HNSCC cell line.....	38
3.1 Introduction.....	38
3.2 UCSF500 analysis in parental and cetuximab-resistant PE/CA-PJ49 cells.....	38
3.3 Unique mutations identified in cetuximab-resistant PE/CA-PJ49 cells.....	39
3.4 Conclusions and future directions.....	43
3.4 Tables.....	45
Chapter 4: Materials and Methods.....	46
References.....	53

List of Figures

Figure 2.1. Cell line models of acquired cetuximab resistance exhibit increased IL-6 secretion.....	27
Figure 2.2. Cetuximab-resistant PE/CA-PJ49 cells are cross-resistant to EGFR-targeted TKIs.....	28
Figure 2.3. Cetuximab-resistant PE/CA-PJ49 cells are not resistant to cisplatin and CBL0137.....	29
Figure 2.4. Addition of recombinant IL-6 does not promote cetuximab resistance in PE/CA-PJ49 parental cells.....	30
Figure 2.5. siRNA-mediated knockdown of <i>IL6</i> does not impact cetuximab response in PE/CA-PJ49 parental and Ctx ^R cells.....	31
Figure 2.6. siRNA-mediated knockdown of <i>IL6R</i> does not impact cetuximab response in PE/CA-PJ49 parental and Ctx ^R cells.....	32
Figure 2.7. siRNA-mediated knockdown of <i>IL6ST</i> does not impact cetuximab response in PE/CA-PJ49 parental and Ctx ^R cells.....	33
Figure 2.8. Pharmacological inhibition of the IL-6 pathway does not impact cetuximab response in PE/CA-PJ49 parental and Ctx ^R cells.....	34
Figure 2.9. Expression of components of the IL-6 pathway are altered in HNSCC cells that have acquired resistance to cetuximab.....	35
Figure 2.10. IL-6 signaling is impaired in PE/CA-PJ49 Ctx ^R cells.....	36
Figure 2.11. Phosphorylation of STAT3 is induced in PE/CA-PJ49 cells treated with rhOSM, but not rhIL6.....	36
Figure 2.12. <i>IL6</i> mRNA expression is increased in Ctx-treated PE/CA-PJ49 parental cells.....	37

List of Tables

Table 3.1. SNVs and indels identified in all PE/CA-PJ49 parental and Ctx ^R cell lines.....	45
Table 3.2. SNVs and indels unique to individual cell lines.....	45
Table 4.1. qPCR primers.....	48

Chapter 1: Introduction

1.1 HNSCC incidence and etiology

Head and neck cancer, which arises in the oral cavity, larynx, and pharynx, is the sixth most common cancer worldwide [1,2]. The majority (~90%) of head and neck tumors are squamous cell carcinomas (HNSCC) [1,3]. Each year, over half a million patients are diagnosed with HNSCC, and despite aggressive therapy, the five-year survival rate for patients with this cancer has hovered around 50% for decades [1,4–7].

The overall incidence of HNSCC has declined in recent decades, due at least in part to a reduction in tobacco use in this time period [1]. However, behavioral and environmental factors that increase the risk of developing HNSCC persist worldwide, with the use of tobacco, alcohol (which acts synergistically with tobacco), and betel nuts leaving a substantial population at risk for developing carcinogen-induced HNSCC [1]. Moreover, the overall decrease in HNSCC incidence masks an increase in human papillomavirus (HPV)-associated HNSCC [1,8].

HPV-associated head and neck tumors, which occur primarily in the oropharynx [1,3,8], arise following infection with high-risk types of human papillomavirus (HPV), particularly HPV-16 [1,8]. Expression of the viral proteins E6 and E7 promote tumorigenesis primarily by inducing degradation of the tumor suppressor proteins p53 and retinoblastoma protein (pRb), respectively [1,8]. Patients with HPV-positive HNSCC are younger, on average, and have an improved prognosis compared to patients with HPV-negative HNSCC [1,9]. The improved prognosis is thought to be due not to the younger average age of patients with HPV-associated HNSCC, but to the improved response to chemoradiotherapy in HPV-positive tumors [8].

1.2 Current treatment strategies in HNSCC

Despite the differences between HPV-positive and -negative HNSCC, including in mechanisms of tumorigenesis, response to chemoradiotherapy, and prognosis, there are currently no FDA-approved therapies specific to either HPV-positive or -negative HNSCC. This may change in the near future, as clinical trials enrolling only HPV-positive or -negative HNSCC are being designed based on the results of studies uncovering further differences between HPV-positive and -negative HNSCC and identifying potential therapeutic targets in their respective cohorts. These studies include a recent comprehensive genomic analysis of 279 HNSCC tumors by The Cancer Genome Atlas (TCGA) Network that incorporated a comparison between HPV-positive and -negative HNSCC tumors [10].

Currently, although the prescribed treatment for HNSCC varies based on tumor stage and anatomical location, platinum-based chemotherapy, radiation, and/or surgery are commonly employed [1,6,7,10–15]. In addition, the immune checkpoint inhibitors nivolumab (Opdivo) and pembrolizumab (Keytruda), both PD-1-targeted monoclonal antibodies, were FDA approved for the treatment of HNSCC in 2016 [3]. To date, the only oncogene-targeted agent that is FDA approved for the treatment of HNSCC is cetuximab (Ctx), a monoclonal antibody that targets the receptor tyrosine kinase (RTK) epidermal growth factor receptor (EGFR; also referred to as ErbB1), which is overexpressed in up to 90% of HNSCC tumors [5,12,16–18].

1.3 EGFR signaling and alterations in cancer

Activation of EGFR occurs when one of its seven ligands binds to its extracellular domain and elicits a conformational change that enables dimerization [19–22]. EGFR can dimerize with other HER family members or with non-HER family RTKs, including AXL, and

the formation of dimers with different partners can modulate the outcome of EGFR activation [23–25]. Dimerization facilitates allosteric activation of the kinase domains of the participating receptors, promoting transphosphorylation of tyrosine residues in the intracellular domain and creating binding sites for downstream effectors, facilitating their activation [20,21,24]. Among the signaling pathways downstream of EGFR that have been shown to mediate EGFR-induced transformation are the phosphoinositide 3-kinase/Akt/mechanistic target of rapamycin (PI3K/Akt/mTOR), RAS/RAF/mitogen-activated protein kinase kinase/extracellular signal-regulated kinase (RAS/RAF/MEK/ERK), and Janus kinase/signal transducer and activator of transcription (JAK/STAT) pathways [19,25–29]. The ability of EGFR to activate these signaling pathways is co-opted by cancer cells, particularly those in which EGFR is overexpressed and/or mutated, to drive tumorigenesis, to promote tumor cell survival and metastasis, to enable immune evasion, and to mediate resistance to chemotherapy.

Aberrant activation of EGFR occurs in many cancer types, although the alterations that lead to this hyperactivation vary. Some cancers exhibit overexpression and/or hyperactivation of wild-type EGFR, while activating mutations are observed in others [19,25,30]. Activating mutations, sometimes co-occurring with amplification of the *EGFR* gene, have been observed in non-small cell lung cancer (NSCLC) and glioblastoma [25,31–33]. Oncogenic fusion proteins containing the N-terminal domain of EGFR were also recently identified in lung adenocarcinoma [34]. In HNSCC, activating mutations in *EGFR* are rarely observed, but amplification of wild-type *EGFR* occurs and often results in overexpression of the EGFR protein, which serves as an oncogenic driver [19,24,25,30,35]. Transcriptional upregulation of *EGFR* in the absence of gene amplification has also been reported in HNSCC [25]. EGFR overexpression occurs in up to 90%

of HNSCC tumors, and EGFR has been established as an oncogenic driver in this disease [24,25,36].

1.4 Cetuximab: An EGFR-targeted therapy used to treat HNSCC

Cetuximab (Erbix) is a human-mouse chimeric monoclonal immunoglobulin G1 (IgG1) antibody that recognizes the extracellular domain of EGFR [17,37–39]. Binding of cetuximab to EGFR prevents ligand binding and activation of the receptor, thereby abrogating EGFR signaling [40]. Cetuximab also triggers internalization of EGFR, resulting in a reduction of cell-surface EGFR levels, and, often, degradation of the receptor [5]. In addition, as an IgG1 monoclonal antibody and, as such, can induce antibody-dependent cell-mediated cytotoxicity (ADCC) [11,38]. In ADCC, the low affinity immunoglobulin gamma Fc region receptor III-A (FcγRIIIA; CD16) on natural killer cells binds to the constant region of IgG1-isotype antibodies. This antibody-NK cell interaction triggers the release of NK cell proteins that induce tumor cell lysis [14,15,41,42].

Cetuximab was first approved for the treatment of HNSCC by the FDA in 2006, when the results of a Phase 3 clinical trial comparing cetuximab plus radiotherapy with radiotherapy alone in a cohort of 424 patients with locoregionally advanced HNSCC were reported [13]. This clinical trial demonstrated that addition of cetuximab to high-dose radiotherapy improved locoregional control, overall survival, and progression-free survival compared to high-dose radiotherapy alone [13]. Also in 2006, cetuximab was approved as a single agent for the treatment of patients with recurrent/metastatic HNSCC whose tumors had previously progressed on platinum-based chemotherapy [43]. (Notably, the response rate to single-agent cetuximab in this trial was 13% [43].) Subsequently, cetuximab was FDA approved in combination with

platinum-based chemotherapy based on results from a clinical trial in which 442 patients with recurrent/metastatic HNSCC were assigned to be treated with cisplatin or carboplatin plus fluorouracil alone or in combination with cetuximab [11]. The addition of cetuximab to this chemotherapy regimen improved overall survival compared to chemotherapy alone [11].

It should be noted that, while cetuximab has been shown to improve response in combination with chemotherapy in HNSCC, other EGFR inhibitors have not fared as well in clinical trials in this disease, despite a number of studies demonstrating that erlotinib and panitumumab are effective in preclinical models of HNSCC [11,25,36,44,45]. It has been suggested, though not proven, that the enhanced clinical efficacy of cetuximab compared to other EGFR inhibitors tested in HNSCC may be explained, at least in part, by its ability to promote immune-mediated tumor clearance via induction of ADCC [44,45]. (Panitumumab, as an IgG2-isotype antibody, is less effective at inducing natural killer cell-mediated ADCC than cetuximab [26,45,46].)

1.5 Challenges in using cetuximab to treat HNSCC

Despite extensive evidence supporting EGFR as a therapeutic target in HNSCC, the response rate for single-agent cetuximab is below 20% in this disease [43,47], and therapy-resistant tumors arise in the majority of cetuximab-treated HNSCC patients [38]. Identification and targeting of pathways that mediate intrinsic and acquired cetuximab resistance could augment the effectiveness of treatment with this drug.

An ongoing challenge in the treatment of HNSCC is the lack of a predictive biomarker(s) for response to cetuximab. Because cetuximab targets EGFR, it was initially hypothesized that high tumoral expression of EGFR would identify tumors most likely to respond to cetuximab;

however, this has not proven to be the case [48–50]. Looking to colorectal cancer, another malignancy for which cetuximab has been FDA approved, tumors harboring activating mutations in *KRAS*, *NRAS*, or *BRAF* are often resistant to cetuximab, and mutations in these genes serve as a negative predictive biomarker for cetuximab response [27,48,51]. In HNSCC, however, activating mutations in *KRAS*, *NRAS*, and *BRAF* are rarely observed, and though activating mutations in *HRAS* have been implicated in cetuximab resistance in HNSCC [52,53], *HRAS* alterations are observed in only 5% of HNSCC tumors and its robustness as a negative predictive biomarker remains unproven [10]. Identification of a predictive biomarker(s) could improve outcomes by enabling identification of a subset of patients whose tumors are likely (or unlikely) to respond to cetuximab. Results of a recent clinical trial designed to identify potential predictive biomarkers of response to cetuximab-containing therapy in HNSCC prompted the project that constitutes the bulk of my dissertation and will be discussed in Chapter 2 [48].

Acquired resistance to cetuximab is another major obstacle in the effective treatment of HNSCC. Even in tumors that initially respond to cetuximab-containing therapy, acquired resistance to cetuximab emerges in the majority of cases, and there are currently no therapeutic avenues to overcome resistance once it develops.

Mechanisms of resistance to cetuximab are varied, but generally promote resistance by restoring activation of the oncogenic signaling pathways downstream of EGFR, often via compensatory activation of alternative receptors and/or activating mutations in components of these downstream signaling pathways.

Increased expression and activation of alternative receptor tyrosine kinases (RTKs) is frequently observed in the context of EGFR inhibition and is a common mechanism of resistance to cetuximab. Compensatory activation of not only human epidermal growth factor receptor

(HER)2 and HER3, two other members of the HER family of RTKs, but also non-HER family RTKs, such as MET and AXL, has been implicated in cetuximab resistance [54–56].

We recently reported activation of alternative RTKs in cetuximab-resistant clones derived from three different cetuximab-sensitive HNSCC cell lines (Cal33, FaDu, and PE/CA-PJ49) [56]. Though the specific RTKs activated varied among the cell lines, each cetuximab-resistant clone exhibited increased activation of alternative RTKs compared to the parental cells from which they were derived. The cetuximab-resistant cells also exhibited increased expression of the bromodomain and extra-terminal (BET) family member bromodomain-containing protein 4 (BRD4), an epigenetic ‘reader’ protein that had previously been shown to promote transcription of RTKs [56–58]. Treatment of the cetuximab-resistant cells with JQ1, a BET bromodomain inhibitor that potently and selectively targets BRD4, re-sensitized cetuximab-resistant FaDu and PE/CA-PJ49 to cetuximab [56,59]. Re-sensitization to cetuximab corresponded with a decrease in RTK expression in JQ1-treated cetuximab-resistant HNSCC cells [56]. Thus, BRD4 inhibition may be a viable therapeutic strategy to target multiple RTKs that have been implicated in cetuximab resistance.

Downstream of EGFR, alterations in the PI3K/Akt/mTOR pathway, particularly activating mutations in *PIK3CA*, have been implicated in resistance to cetuximab in HNSCC [52,60], and co-targeting with inhibitors of the PI3K/Akt/mTOR has been shown to enhance the anti-tumor effects of cetuximab in preclinical HNSCC models [5,18,60]. Previous work from our laboratory has shown that the oncogenic transcription factor STAT3 is aberrantly activated in cell line models of acquired resistance [61]. In addition, the ability of cetuximab to inhibit cell proliferation was shown to be enhanced in HNSCC cells in which STAT3 was knocked down [62].

Although a number of mechanisms of resistance to cetuximab have been identified, these efforts have not yet led to an FDA-approved treatment strategy to prevent and/or overcome cetuximab resistance. To address this unmet need and the distinct, yet related challenge of identifying a predictive biomarker that can detect tumors that are intrinsically resistant to cetuximab, we assessed the role of interleukin 6 (IL-6) signaling in acquired resistance of cetuximab. Our findings are presented in Chapter 2.

Chapter 2: Interleukin 6 is increased in preclinical HNSCC models of acquired cetuximab resistance, but is not required for maintenance of resistance

2.1 Introduction

As discussed in Chapter 1, there are currently no predictive biomarkers to guide selection of HNSCC patients whose tumors are likely to respond (or not respond) to cetuximab. Expression of EGFR itself cannot predict whether an HNSCC tumor will respond to cetuximab [48–50], and activating mutations in *KRAS*, *NRAS*, and *BRAF* that serve as predictive biomarkers of resistance to cetuximab in colorectal cancer occur at very low frequencies in HNSCC and thus cannot serve as predictive biomarkers in this disease [27,48,51]. Use of a predictive biomarker(s) could improve outcomes by informing selection of patients to be treated with cetuximab, allowing clinicians to provide cetuximab to HNSCC patients who are likely to benefit from treatment with cetuximab without subjecting patients whose tumors are unlikely to respond to cetuximab to treatment with this drug. Stratifying patients in this manner requires the identification of a biomarker(s) whose expression can reliably predict which HNSCC tumors will respond to cetuximab treatment.

To this end, a recent Phase II clinical trial sought to identify serum biomarkers that could predict resistance to a combination of cetuximab and the Src family kinase inhibitor dasatinib in HNSCC patients whose tumors had previously progressed on cetuximab-containing therapy [48]. In this trial, serum was collected from 13 patients before and after treatment with a combination of cetuximab and dasatinib, and the concentrations of four candidate biomarkers (hepatocyte

growth factor [HGF], interleukin 6 [IL-6], transforming growth factor alpha [TGF- α], and vascular endothelial growth factor [VEGF]) were compared in the pre- and post-treatment samples [48]. Of the four candidate serum biomarkers, only IL-6 levels were shown to be correlated with resistance to the combination of cetuximab and dasatinib [48], identifying high serum IL-6 as a potential predictive biomarker of resistance to cetuximab-containing therapy in HNSCC.

First discovered as a factor that promotes immunoglobulin production by B cells (and originally referred to as B-cell stimulatory factor-2) [63], IL-6 has since been frequently implicated in cancer due to its ability to activate oncogenic intracellular signaling pathways in cancer cells and regulate immunosuppression in the tumor microenvironment [64,65].

IL-6 is a member of a family of cytokines that includes IL-11, IL-27, leukemia inhibitory factor (LIF), and oncostatin M (OSM), among others, all of which utilize the common signal transducing receptor glycoprotein 130 (gp130) [64,66–69]. The cytokines achieve specificity by binding not to gp130, but to unique cytokine receptors that subsequently dimerize with gp130 [66,68,69].

IL-6 promotes activation of its receptor via two pathways, referred to as classic and trans-signaling [67–69].

In classic IL-6 signaling, IL-6 binds to the membrane-bound IL-6 receptor- α (IL-6R α), thus inducing formation of a heterohexameric complex consisting of two molecules each of IL-6, IL-6R α , and gp130 [64,66]. Janus kinase (JAK) proteins bind to the Box1 and Box2 domains in the intracellular portion of gp130, leading to JAK-mediated phosphorylation of gp130 at several tyrosine residues, including four C-terminal residues that serve as docking sites for signal transducer and activator of transcription 3 (STAT3) [63,69]. Once bound to gp130, STAT3 is

phosphorylated by JAKs at tyrosine 705, leading to STAT3 dimerization and nuclear translocation, followed by STAT3-mediated transcription of target genes [65,69]. The IL-6/IL-6R α /gp130 complex can also activate the PI3K/Akt/mTOR and RAS/RAF/MEK/ERK pathways [67].

In IL-6 trans-signaling, soluble IL-6R α (sIL-6R α), rather than membrane-bound IL-6R α , binds to IL-6. sIL-6R α can be generated by alternative splicing of *IL6R* mRNA or, more often, by cleavage of membrane-bound IL-6R α by disintegrin and metalloproteinase domain-containing protein 10 (ADAM10) or ADAM17 [65,67,68]. When IL-6 binds with sIL-6R α , this complex is then able to bind to and induce the dimerization of membrane-bound gp130, leading to the activation of downstream signaling pathways (as described above for classic IL-6 signaling pathways) [65,67]. While gp130 is ubiquitously expressed, IL-6R α is expressed in only a limited number of cell types [67,68]. Thus, trans-signaling via sIL-6R α allows IL-6 to act on cells with limited or absent IL-6R α expression. IL-6 trans-signaling can be negatively regulated by soluble gp130 (sgp130), which is generated by alternative splicing of *IL6ST* mRNA [67]. Soluble gp130 competes with membrane-bound gp130 for binding to the IL-6–sIL-6R α complex, thereby inhibiting IL-6 trans-signaling, but not the classic IL-6 signaling pathway [68].

As described in Chapter 1 and above, both EGFR and IL-6 promote activation of the JAK/STAT, PI3K/Akt/mTOR, and RAS/RAF/MEK/ERK pathways [67]. Thus, EGFR and IL-6 signaling converge on several oncogenic signaling pathways, providing a plausible mechanism by which IL-6 could oppose the antitumor effects of cetuximab: maintaining activation of these pathways in the context of EGFR inhibition. Indeed, previous investigations have demonstrated that downstream mediators of IL-6 signaling, particularly STAT3 and components of the PI3K/Akt pathway, can promote resistance to EGFR-targeted therapies [17,60,61].

IL-6 itself was implicated in cetuximab resistance in a 2010 study focusing on pharyngeal cell lines [17]. In this study, cetuximab-resistant cells generated by treating parental (cetuximab-sensitive) FaDu cells with increasing concentrations of cetuximab exhibited increased *IL6* expression and STAT3 phosphorylation compared to the parental cells from which they were derived [17]. The authors also showed that treating parental FaDu cells with cetuximab for 48 hours reduced the number of viable cells in a dose-dependent manner, and that adding recombinant IL-6 tempered the effects of cetuximab on cell number [17]. In addition, in three pharyngeal cell lines (including FaDu), combining an IL-6 targeted monoclonal antibody with cetuximab more effectively reduced viable cell number than cetuximab alone (although it is unclear whether IL-6 inhibition alone had an impact, as these data were not reported) [17]. These data demonstrate that increased *IL6* expression is correlated with cetuximab resistance in an HNSCC cell line and suggest that IL-6 inhibition may enhance cetuximab response [17].

Another study, published in 2013, provided further evidence that IL-6 may play a role in resistance to EGFR-targeted therapies in HNSCC [70]. In this study, IL-6 was among the pro-inflammatory cytokines whose expression was increased upon treatment of HNSCC cell lines with the EGFR-targeted tyrosine kinase inhibitor erlotinib [70]. The authors found that treatment with recombinant IL-6 protected cells from erlotinib-induced cytotoxicity in clonogenic survival assays [70]. Moreover, treating mice bearing HNSCC cell line xenografts with a combination of erlotinib and the IL-6R α -targeted monoclonal antibody tocilizumab further reduced tumor volume compared to treatment with erlotinib alone [70]. Notably, treatment with tocilizumab alone did not have a significant impact on tumor volume [70]. This study provided further evidence that IL-6 may play a role in resistance to EGFR inhibition in HNSCC.

These studies reporting that inhibition of the IL-6 pathway can enhance the antitumor effects of EGFR inhibitors suggest that IL-6 is not only a potential predictive biomarker of cetuximab resistance in HNSCC, but also a plausible therapeutic target, particularly in the context of cetuximab-resistant disease. Drugs targeting IL-6 and the IL-6 receptor, as well as downstream components of the IL-6 pathway, have been developed. Though none have been FDA approved for the treatment of HNSCC, some have been FDA approved for other indications [71–73]. Siltuximab, sirukumab, olokizumab, clazakizumab, and MEDI5117 are anti-IL-6 monoclonal antibodies [65,74]. Tocilizumab and sarilumab are monoclonal antibodies that target IL-6R α [65,67]. These antibodies inhibit both the classic and trans-signaling pathways [65,67]. In contrast, the gp130–Fc fusion protein olamkicept inhibits IL-6 trans-signaling but not the classic signaling pathway [65,67]. Tofacitinib, ruxolitinib, pacritinib, and AZD1480 are small-molecule tyrosine kinase inhibitors that target JAKs, preventing phosphorylation of STAT3 [65,75,76]. C188-9, OPB-31121, OPB-51602, and other Src homology domain 2 (SH2) domain inhibitors interfere with STAT3 dimerization [65]. The STAT3 antisense oligonucleotide AZD9150 binds to and causes the destruction of *STAT3* mRNA, thus decreasing STAT3 expression [65,77]. The cyclic STAT3 decoy contains a nucleotide sequence derived from the promoter of the STAT3 target gene *FOS*. This decoy competitively inhibits STAT3 binding to genomic response elements in the promoter regions of target genes [65,78]. Thus, there exist many therapeutic strategies to inhibit the IL-6 signaling if this pathway proves to be a therapeutic target in cetuximab-resistant HNSCC.

Based on the results of the Phase II trial of cetuximab and dasatinib in HNSCC [48], as well as preclinical evidence supporting a role for IL-6 in cetuximab resistance, we investigated the role of the IL-6 pathway in preclinical HNSCC models of acquired cetuximab resistance. We

hypothesized that IL-6 would promote cetuximab resistance in HNSCC cells and that inhibiting the IL-6 pathway in a cell line model of acquired cetuximab resistance would restore sensitivity to cetuximab. Instead, we found that, despite increased IL-6 secretion in our cetuximab-resistant (Ctx^R) models, treatment of the parental (cetuximab-sensitive) cells with exogenous IL-6 did not promote cetuximab resistance, nor did inhibition of components of the IL-6 pathway restore cetuximab sensitivity in the Ctx^R cells. Further, we found that expression of *IL6R*, which encodes the IL-6 receptor subunit IL-6R α , was substantially reduced in the Ctx^R cells compared to parental cells, and that Ctx^R cells did not respond to IL-6 stimulation with an increase in phosphorylation of STAT3 at Y705. Thus, though IL-6 secretion is correlated with cetuximab resistance in the PE/CA-PJ49 Ctx^R models, IL-6 is not required for the maintenance of cetuximab resistance in these cells, and targeting the IL-6 pathway may not restore cetuximab sensitivity even in cetuximab-resistant tumors that exhibit increased expression of this cytokine.

2.2 Results

IL-6 secretion is increased in cell line models of acquired cetuximab resistance.

We recently reported the generation of cell line models of acquired cetuximab resistance derived from the parental HNSCC cell line PE/CA-PJ49 [56]. We reported that in these cell lines, an increase in expression of alternative receptor tyrosine kinases (RTKs), including AXL and MET, promotes resistance to EGFR inhibition. Expression of these alternative RTKs was driven by upregulation of the transcriptional co-activator bromodomain-containing protein-4 (BRD4), and targeting BRD4 was able to restore cetuximab sensitivity in these cells [56]. Whether additional alterations in these model cell lines contribute to cetuximab resistance

remains unexplored. Thus, we utilized these models to assess the role of IL-6 in acquired resistance to cetuximab.

We first confirmed that these PE/CA-PJ49 Ctx^R cells maintained resistance to cetuximab in 96-hour dose-response (**Fig. 2.1A**) and 12-day clonogenic survival (**Fig. 2.1B**) assays. Of note, PE/CA-PJ49 Ctx^R cells were also resistant to the EGFR-targeted tyrosine kinase inhibitor (TKI) erlotinib and the dual EGFR/HER2-targeted TKIs afatinib and lapatinib (**Fig. 2.2**), but remained sensitive to cisplatin and CBL0137, a novel anti-cancer agent targeting the facilitates chromatin transcription (FACT) complex [79,80] (**Fig. 2.3**), suggesting cross-resistance to EGFR targeting but not general treatment resistance.

Previous studies focusing on mechanisms of resistance to cetuximab and other EGFR-targeted therapies have demonstrated that EGFR inhibitor-resistant cells secrete increased levels of IL-6 compared to sensitive cells [17,61,81]. Consistent with these reports [17,61], *IL6* mRNA expression was increased in the PE/CA-PJ49 cetuximab-resistant (Ctx^R) cells compared to the parental cells from which they were derived (**Fig. 2.1C**). To measure secreted IL-6 in our models of acquired cetuximab resistance, PE/CA-PJ49 parental and Ctx^R cells were plated in serum- and antibiotic-free media and an enzyme-linked immunosorbent assay (ELISA) was performed on cell culture supernatants collected after 72 hours. As shown in **Fig. 2.1D**, IL-6 was increased in the cell culture supernatants of Ctx^R cells compared to parental cells. These results suggested that IL-6 might play a role in acquired resistance to cetuximab in the PE/CA-PJ49 Ctx^R models and provided the impetus for further investigation of the IL-6 pathway.

Recombinant IL-6 does not confer cetuximab resistance in parental PE/CA-PJ49 cells.

Because we observed an increase in IL-6 secretion in the cetuximab-resistant PE/CA-PJ49 cells compared to parental cells, and because IL-6 and its downstream effector STAT3 have been previously implicated in cetuximab resistance [17,61], we sought to determine whether addition of recombinant human IL-6 (rhIL6) would abrogate the growth inhibitory effects of cetuximab in PE/CA-PJ49 parental cells.

Before testing the impact of rhIL6 addition on cetuximab response in the PE/CA-PJ49 parental cells, we first determined whether rhIL6 was able to activate signaling downstream of the IL-6 receptor. The media on PE/CA-PJ49 parental cells was replaced with DMEM (no FBS) or DMEM supplemented with 10% FBS. After 4 hours, the cells were treated with 50 ng/mL rhIL6 for 15 minutes or 4 hours. Phosphorylation of STAT3 at tyrosine 705 (P-STAT3^{Y705}) was increased upon addition of rhIL6 in both the no FBS and 10% FBS conditions, while total STAT3 levels remained stable (**Fig. 2.4A**), demonstrating that rhIL6 can indeed activate the JAK/STAT pathway in these cells even in the presence of serum. To assess the impact of rhIL6 on cetuximab response, we treated the cells for 96 hours with 100 nM Ctx, 50 ng/mL rhIL6, or the combination of Ctx and rhIL6, then stained the cells with crystal violet (**Fig. 2.4B**). The addition of rhIL6 did not prevent cetuximab-induced growth inhibition in the PE/CA-PJ49 parental cells (**Fig. 2.4B,C**). These findings indicate that exogenous IL-6 alone cannot promote cetuximab resistance in this model cell line.

Inhibition of the IL-6 pathway does not impact cetuximab response in PE/CA-PJ49 parental and Ctx^R cells.

Although addition of recombinant IL-6 did not promote cetuximab resistance in PE/CA-PJ49 parental cells, this did not rule out the possibility that IL-6 played a role in the maintenance of cetuximab resistance in the Ctx^R cell lines. This was an appealing prospect because if IL-6 were required to maintain cetuximab resistance, then targeting the IL-6 pathway could be used to restore cetuximab sensitivity in these cell lines, and, potentially, in cetuximab-resistant HNSCC tumors. To determine whether inhibiting the IL-6 pathway could restore cetuximab sensitivity in the PE/CA-PJ49 Ctx^R cell lines, we used both genetic and pharmacologic approaches to inhibit components of the IL-6 pathway alone and in combination with cetuximab.

To determine the impact of *IL6* knockdown on cetuximab response, we first confirmed that the siRNAs targeting *IL6* reduced *IL6* mRNA expression by transfecting PE/CA-PJ49 parental cells with 10 nM nontargeting (nt) siRNA or one of two distinct *IL6*-targeted siRNAs (siIL6 A and B). After 96 hours, quantitative reverse transcription PCR (qPCR) was performed to assess *IL6* mRNA levels. Cells transfected with either siIL6 A or siIL6 B exhibited a substantial reduction in *IL6* mRNA levels compared to nt-transfected cells (**Fig. 2.5A**).

We next plated PE/CA-PJ49 parental and Ctx^R cells at a low density to conduct clonogenic survival assays. Cells were transfected with 10 nM nt siRNA, siIL6 A, or siIL6 B and treated the next day (and every four days thereafter) with vehicle (PBS) or 100 nM Ctx. After 12 days of treatment (13 days post-transfection), the colonies were stained with crystal violet. As expected, PE/CA-PJ49 parental cells were sensitive to cetuximab (**Fig. 2.5B**). Transfection with siIL6 itself reduced the number of colonies per well in the parental and Ctx^R cells, and the combination of cetuximab and siIL6 had an additive effect in parental cells. However, siIL6-

transfected Ctx^R cells treated with vehicle and cetuximab were indistinguishable, demonstrating that the Ctx^R cells remain resistant to cetuximab even when *IL6* expression is greatly reduced.

Next, we examined the impact of knocking down other components of the IL-6 pathway on cetuximab response. IL-6 signals through a receptor complex consisting of interleukin-6 receptor alpha (IL-6R α , encoded by *IL6R*) and glycoprotein 130 (gp130, encoded by *IL6ST*). IL-6 signaling is initiated when IL-6 binds to IL-6R α and the IL-6/IL-6R α complex binds to gp130. Subsequent dimerization of gp130 leads to the formation of a heterohexameric signaling complex that recruits JAK proteins, leading to phosphorylation and nuclear localization of STAT3 [73,82–85]. Both IL-6R α and gp130, in addition to IL-6, are required to initiate IL-6 signaling [73,83,84]; thus, if IL-6 signaling is required to maintain cetuximab resistance in the PE/CA-PJ49 Ctx^R cells, inhibition of either co-receptor would be expected to restore cetuximab sensitivity in these cells. Transfection of PE/CA-PJ49 parental cells with siIL6R (**Fig. 2.6**) or siIL6ST (**Fig. 2.7**) substantially reduced the mRNA levels of their respective targets in PE/CA-PJ49 parental cells. However, as observed when *IL6* was knocked down, neither siIL6R nor siIL6ST restored cetuximab sensitivity in the Ctx^R cell lines (**Fig. 2.6 and 2.7**).

To corroborate the results we obtained using siRNAs with a more clinically relevant agent, we used tocilizumab (TCZ), an IL-6R α -targeted monoclonal antibody that is FDA approved for the treatment of rheumatoid arthritis and chimeric antigen receptor (CAR) T cell-induced cytokine release syndrome. To select a concentration of TCZ for use in subsequent experiments, we serum starved PE/CA-PJ49 parental cells for 2 hours, then pre-treated the cells with vehicle (PBS) or increasing concentrations of TCZ for 2 hours before treating the cells for 15 minutes with 50 ng/mL rhIL6. We found that 100 nM TCZ was sufficient to block rhIL6-induced STAT3 phosphorylation (**Fig. 2.8A**) and selected 1 μ M TCZ as the concentration for

subsequent experiments because a further decrease in STAT3 phosphorylation was observed in cells treated with this concentration.

To assess the impact of TCZ on cetuximab response in the PE/CA-PJ49 parental and Ctx^R cells, we again plated the cells at a low density, then treated the cells with vehicle (PBS), 100 nM Ctx, 1 μ M TCZ, or the combination of Ctx and TCZ, replacing media plus drug(s) every four days, for a total of 12 days of treatment (**Fig. 2.8B,C**). In cells treated with cetuximab alone, a substantial decrease in crystal violet-stained material was observed in PE/CA-PJ49 parental cells, but not Ctx^R cells. Treatment with TCZ, whether alone or in combination with cetuximab, did not have an impact on colony formation in parental or Ctx^R cells (**Fig. 2.8B,C**).

Despite a substantial increase in IL-6 levels (both mRNA expression and secreted cytokine) in the Ctx^R cell lines compared to PE/CA-PJ49 parental cells, inhibition of components of the IL-6 pathway using both genetic (siRNA) and pharmacological (TCZ) methods did not impact cetuximab response in the Ctx^R cells. Together, these results suggest that IL-6 signaling is not required for maintenance of cetuximab resistance in these models.

Expression of components of the IL-6 pathway are altered in HNSCC cells that have acquired resistance to cetuximab.

Though IL-6 levels are increased in PE/CA-PJ49 Ctx^R cells compared to parental cells (**Fig. 2.1**), treatment of parental cells with rhIL6 did not promote cetuximab resistance (**Fig. 2.4**), and inhibition of the IL-6 pathway failed to reverse cetuximab resistance in the Ctx^R cells (**Fig. 2.5-2.8**). Seeking an explanation for this discrepancy, we analyzed expression of gp130 and IL-6R α , both of which are required for IL-6 signal transduction, in parental and Ctx^R PE/CA-PJ49 cells.

Expression of gp130 (encoded by the *IL6ST* gene) was evaluated by qPCR and immunoblot analysis and found to be increased at both the mRNA (**Fig. 2.9A**) and protein (**Fig. 2.9C,D**) levels in Ctx^R cells compared to parental PE/CA-PJ49 cells. In contrast, mRNA expression of *IL6R* (the gene encoding IL-6R α) was decreased in PE/CA-PJ49 Ctx^R cells compared to parental cells (**Fig. 2.9B**). This raises the question of whether IL-6 signaling is functionally intact in the PE/CA-PJ49 Ctx^R cells.

IL-6 signaling is impaired in PE/CA-PJ49 Ctx^R cells.

Although both IL-6 and gp130 levels were increased in Ctx^R PE/CA-PJ49 cells, IL-6R α levels were decreased in these cells compared to parental cells, revealing a disconnect among the components of the IL-6 signaling pathway. This discrepancy led us to examine the net impact of these alterations on downstream components of the IL-6 signaling pathway in the PE/CA-PJ49 Ctx^R cells.

We compared P-STAT3^{Y705} levels in PE/CA-PJ49 parental and Ctx^R cells and found that the ratio of P-STAT3^{Y705} to total STAT3 was decreased in Ctx^R cells compared to parental cells (**Fig. 2.10A,B**), consistent with impaired IL-6 signaling in the Ctx^R cells. However, because STAT3 phosphorylation is dynamically regulated by a number of kinases and phosphatases, the decrease in P-STAT3^{Y705} in the Ctx^R cells alone does not conclusively demonstrate a defect in IL-6 signaling. Thus, we assessed IL-6 signaling more directly by serum starving parental and Ctx^R PE/CA-PJ49 cells, then treating the cells for 15 minutes with 50 ng/mL rhIL6. Consistent with our findings in **Fig. 2.4A**, addition of rhIL6 stimulated phosphorylation of STAT3 at Y705 in the parental cells. However, no increase in P-STAT3^{Y705} was observed following 15 minutes of rhIL6 treatment in any of the Ctx^R lines (**Fig. 2.10C and 2.11**).

To determine whether this defect was IL-6-specific, we tested whether P-STAT3^{Y705} levels in the Ctx^R cells were increased following treatment with recombinant human leukemia inhibitory factor (rhLIF) or recombinant human oncostatin M (rhOSM). LIF and OSM are IL-6 family cytokines that utilize gp130 for signal transduction, but bind to non-IL-6R α co-receptors to initiate signaling [83]. We serum starved PE/CA-PJ49 parental and Ctx^R cells for 4 hours, then treated the cells for 15 minutes with 50 ng/mL rhIL6 or rhLIF. While rhLIF treatment induced STAT3 phosphorylation at Y705 in the parental and Ctx^R cell lines, rhIL6 increased P-STAT3^{Y705} levels in only the parental cells (**Fig. 2.10C**). Similar results were observed when cells were treated with rhOSM: Serum-starved parental and Ctx^R cell lines all responded to rhOSM treatment with an increase in P-STAT3^{Y705} (**Fig. 2.11**).

PE/CA-PJ49 parental and Ctx^R cell lines all responded to treatment with the IL-6 family cytokines LIF and OSM with an increase in P-STAT3^{Y705}, demonstrating that gp130 and JAK/STAT3 signaling are functionally competent in these cells. In contrast, only the parental cells responded to treatment with rhIL6, suggesting that the decreased *IL6R* expression in the PE/CA-PJ49 Ctx^R cells impacted their ability to mediate IL-6 signaling and providing further evidence that IL-6 is not required for the maintenance of cetuximab resistance in these cells.

2.3 Discussion

Based on evidence in preclinical models and the finding that serum IL-6 was a biomarker of resistance to cetuximab-containing therapy in a Phase II trial [48], we initially hypothesized that IL-6 mediated cetuximab resistance in HNSCC cells and that targeting the IL-6 pathway could overcome cetuximab resistance. Our initial characterization of *IL6* expression and secretion in the PE/CA-PJ49 Ctx^R cells was consistent with a role for IL-6 in cetuximab

resistance, as IL-6 levels were increased in all three Ctx^R models compared to the parental PE/CA-PJ49 cells from which they were derived. However, inhibition of the IL-6 pathway did not restore cetuximab sensitivity in the Ctx^R models, and subsequent analyses revealed that, though parental PE/CA-PJ49 cells responded to IL-6 treatment with an increase in P-STAT3^{Y705}, the Ctx^R cells failed to do so, possibly due to the substantial decrease in expression of *IL6R* in the Ctx^R cells. These cumulative results suggest that, despite an increase in IL-6 secretion in the PE/CA-PJ49 Ctx^R models, IL-6 does not mediate cetuximab resistance in these models.

This project was initiated based on the results of a Phase II clinical trial performed to identify potential predictive biomarkers of response to a combination of cetuximab and dasatinib in HNSCC patients whose tumors had previously progressed on cetuximab-containing therapy [48]. The investigators found that, out of four candidate serum biomarkers, only IL-6 serum levels were shown to be correlated with resistance to the combination of cetuximab and dasatinib [48]. This clinical trial, along with the aforementioned preclinical studies linking IL-6 with resistance to EGFR inhibitors in HNSCC cells [17,70], suggested that IL-6 could be a predictive biomarker of resistance to cetuximab. However, there exists a crucial difference between our study and the clinical trial on which this project was based: While our study focused on cetuximab resistance, the clinical trial focused on the association of IL-6 with resistance to a combination of cetuximab and dasatinib. Taken together, these results suggest that IL-6 might promote resistance to the combination of cetuximab and dasatinib, or to dasatinib alone, but not to cetuximab alone. Further experiments in additional models would be needed to test this.

With regards to the papers by Chen et al. and Fletcher et al., which demonstrated that inhibition of IL-6 signaling could enhance the anti-tumor effects of EGFR inhibitors alone [17,70], any number of factors could explain the discrepancies in our findings – for example, the

findings could simply be cell line-specific. An additional consideration is that, while we focused on the effects of IL-6 inhibition in cells that had already acquired resistance to cetuximab, the cited papers treated EGFR inhibitor-naïve cells with IL-6 inhibitors. Thus, our disparate findings might simply reflect differences in the role of IL-6 upon initial treatment with EGFR inhibitors and after months of treatment with increasing concentrations of the drug. Though we concluded that IL-6 is not required for the maintenance of cetuximab resistance in the PE/CA-PJ49 Ctx^R cells, IL-6 could have played a role in the acquisition of cetuximab resistance. It has previously been shown that erlotinib-induced NF-κB-mediated *IL6* expression promotes survival of non-small cell lung cancer cells treated with this EGFR tyrosine kinase inhibitor, and it was suggested that this adaptive response to erlotinib treatment could ultimately promote acquired resistance to this drug [86]. We observed an increase in *IL6* mRNA expression when parental PE/CA-PJ49 cells were treated with cetuximab for 96 hours (**Fig. 2.12**), suggesting that *IL6* expression is increased in response to cetuximab treatment and that the increase in IL-6 secretion occurs prior to the acquisition of cetuximab resistance in the PE/CA-PJ49 cells. This finding is consistent with the erlotinib-induced increase in IL-6 reported by Fletcher et al. [70]. Given the previously demonstrated role of IL-6 in promoting cell survival upon treatment with EGFR inhibitors [86], future studies may test the hypothesis that cetuximab-induced secretion of IL-6 allows cetuximab-sensitive cells to persist during treatment, enabling the eventual acquisition of resistance by persister cells.

Our conclusion that IL-6 does not promote cetuximab resistance in the PE/CA-PJ49 Ctx^R cells despite an upregulation in *IL6* expression, though initially surprising, is not without precedent. A previous study found that, despite increased secretion of IL-6 in HNSCC cell line models of acquired resistance to cisplatin, IL-6 did not mediate cisplatin resistance in these cells

[87]. Moreover, expression of *IL6R* was decreased in the cisplatin-resistant cells, and the authors speculated that this decrease in *IL6R* expression impaired IL-6 signaling [87]. Thus, in both cetuximab-resistant and cisplatin-resistant HNSCC cells, an increase in IL-6 secretion in conjunction with the emergence of drug resistant cells does not necessarily demonstrate that IL-6 is required for maintenance of drug resistance. It also raises the intriguing question of why *IL6R* expression was decreased in both of these drug resistance models. Was *IL6R* simply a bystander lost during acquisition of drug resistance, or were the decreases in *IL6R* expression due to selective pressure? Examination of these and other possibilities could be addressed in future studies. We emphasize that our conclusion that IL-6 is not required for the maintenance of cetuximab resistance is specific to the PE/CA-PJ49 models used in this study. IL-6 may be involved in the maintenance of acquired resistance in IL-6 signaling-competent cells – indeed, this may explain a discrepancy between our findings and those of Chen et al. [17]. We predict that IL-6 may be dispensable for the maintenance of cetuximab resistance in other cells in which *IL6R* expression is decreased or absent, or in which IL-6 signaling is otherwise impaired. This prediction may be tested in the future.

The inability of the PE/CA-PJ49 Ctx^R cells to activate STAT3 in response to treatment with recombinant IL-6 suggests that the decrease in *IL6R* expression had a functional impact on response to IL-6. Because both IL-6R α and gp130 are required to form functional IL-6 receptors, it is perhaps not surprising that the substantial reduction in IL-6R α levels in PE/CA-PJ49 Ctx^R cells would impede the ability of IL-6 to induce STAT3 phosphorylation (**Fig 5C; S6 Fig**). In light of these findings, the inability of IL-6 pathway inhibition to reverse cetuximab resistance in the Ctx^R cells is not surprising; indeed, the results would have been difficult to interpret had IL-6 inhibition restored cetuximab sensitivity in cells in which IL-6 signaling is

impaired. However, though we hypothesize that the impairment in IL-6 signaling is due the decrease in *IL6R* expression, it could be due to other alterations in the Ctx^R cells. Additional experiments would need to be conducted to conclude that the decrease in IL-6R α levels was responsible for the functional impairment in IL-6 signaling in Ctx^R cells. For example, if overexpressing IL-6R α restored the ability of the Ctx^R cells to phosphorylate STAT3 in response to treatment with IL-6, this would suggest that the impairment in IL-6 signaling was indeed due to the decrease in *IL6R* expression. Moreover, the inability of recombinant IL-6 to activate IL-6 signaling in the Ctx^R cells does not rule out the possibility that IL-6 signals intracellularly, as IL-6 has been shown to activate signaling within endosomes [88]. This may explain an apparent discrepancy in **Fig. 2.5, 2.6, and 2.8**, in which siRNA-mediated knockdown of *IL6* or *IL6R*, but not treatment with the IL-6R α -targeted agent TCZ, reduces colony number in PE/CA-PJ49 parental and Ctx^R cells. Though this does not appear to play a role in the maintenance of cetuximab resistance, since knockdown of *IL6*, *IL6R*, and *IL6ST* did not sensitize the cells to cetuximab, the respective contributions of intracellular and extracellular IL-6 in HNSCC may be a topic of further study.

Notably, our results also do not rule out a potential role for IL-6 in cetuximab resistance in an *in vivo* setting. PE/CA-PJ49 cells do not reliably form xenograft tumors in even the severely immunocompromised NOD *scid* gamma strain of mice, so the experiments described above were conducted exclusively in cell culture or in samples derived from cell lines. These isolated cell culture models lack 3D architecture and components of the tumor microenvironment, including immune cells, which are especially relevant in the context of cetuximab treatment because one of cetuximab's mechanisms of action is immune cell-dependent. Cetuximab is a monoclonal antibody and has been shown to mediate ADCC, a

phenomenon in which immune cells (primarily natural killer cells) recognize and kill cells opsonized by antibodies [15]; thus, impairment of this process could impede the ability of cetuximab to promote immune-mediated tumor cell destruction. An abundance of evidence has established that IL-6 plays many roles in the tumor microenvironment, often as an immunosuppressive cytokine [89,90], and it is tempting to speculate that IL-6 secretion by cetuximab-resistant tumor cells could promote cetuximab resistance by downregulating cetuximab-induced ADCC. Future studies may explore whether IL-6 plays a role in resistance to cetuximab-induced ADCC, perhaps in a tumor/immune cell co-culture model.

IL-6 upregulation has been repeatedly demonstrated in the context of treatment with, and resistance to, cetuximab and other EGFR-targeted therapies [17,48,70,86]. Upon observation that IL-6 secretion was increased in PE/CA-PJ49 Ctx^R cells compared to parental cells, we expected to find that IL-6 mediated cetuximab resistance and that inhibiting the IL-6 pathway would restore cetuximab sensitivity in Ctx^R cells. Instead, we found that the increase in IL-6 secretion by PE/CA-PJ49 Ctx^R cells belied a functional impairment in the IL-6 signaling pathway. These findings demonstrate that, even when IL-6 levels are increased in the context of cetuximab resistance, this does not necessarily indicate that IL-6 mediates cetuximab resistance. This study highlights the importance of differentiating between alterations that are simply correlated with cetuximab resistance and those that play a functional role in maintaining cetuximab resistance in order to identify promising candidates to target to overcome cetuximab resistance.

2.4 Figures

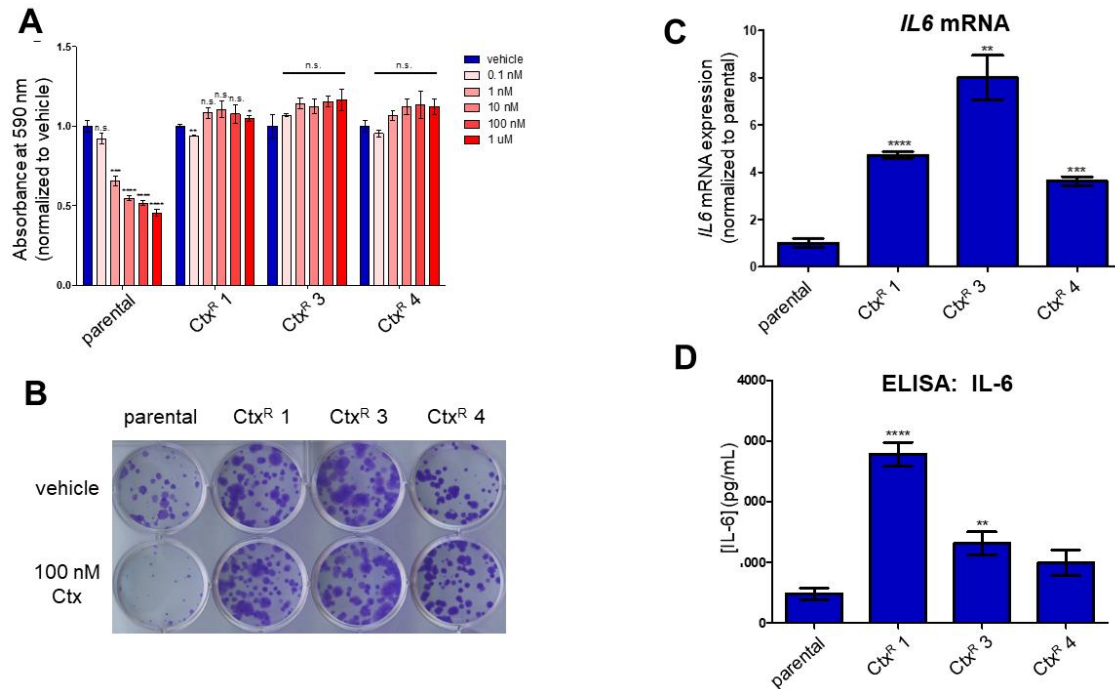


Figure 2.1. Cell line models of acquired cetuximab resistance exhibit increased IL-6 secretion. **A)** PE/CA-PJ49 parental and Ctx^R cells were treated for 96 h with vehicle (PBS) or cetuximab (0.1 nM – 1 μ M), then stained with crystal violet. Student's two-tailed t-test was used to determine whether differences in absorbance at 590 nm were statistically significant (compared to vehicle-treated cells). n=4. **B)** Cells were plated at low density and treated the next day with vehicle (PBS) or 100 nM cetuximab. Cells were stained with crystal violet after 12 days of cetuximab treatment. Media containing vehicle or cetuximab was changed every 4 days. **C)** RNA was extracted from PE/CA-PJ49 parental and Ctx^R cells and qPCR was conducted using the *IL6* primers listed in **Table 4.1** (normalized to *TBP*). n=3. **D)** PE/CA-PJ49 parental cells and Ctx^R cells were plated in serum-free medium. Conditioned medium was collected after 72h and concentration of IL-6 was measured using ELISA. Student's two-tailed t-test was used to determine whether differences in IL6 expression and secreted IL-6 were statistically significant (compared to parental cells). n=4. *p<0.05; **p<0.01; ***p<0.001; ****p<0.0001; n.s., not significant.

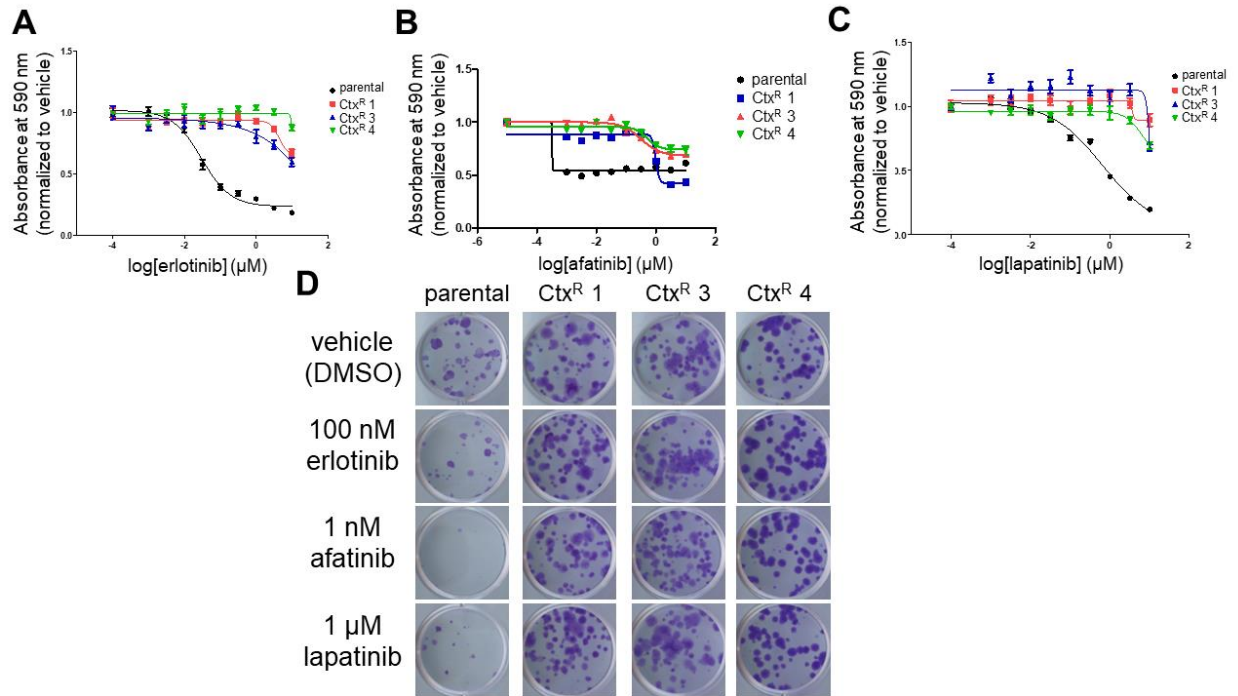


Figure 2.2. Cetuximab-resistant PE/CA-PJ49 cells are cross-resistant to EGFR-targeted TKIs. A,B,C) Erlotinib (A), afatinib (B), and lapatinib (C) dose response assays in PE/CA-PJ49 parental cells and Ctx^R clones treated for 96 h, then stained with crystal violet. n=6. **D)** PE/CA-PJ49 parental cells and Ctx^R clones were plated at low density and treated with vehicle (DMSO), 100 nM erlotinib, 1 nM afatinib, or 1 μM lapatinib, then stained with crystal violet after 12 days of treatment. Media containing vehicle or drug was changed every four days. n=4.

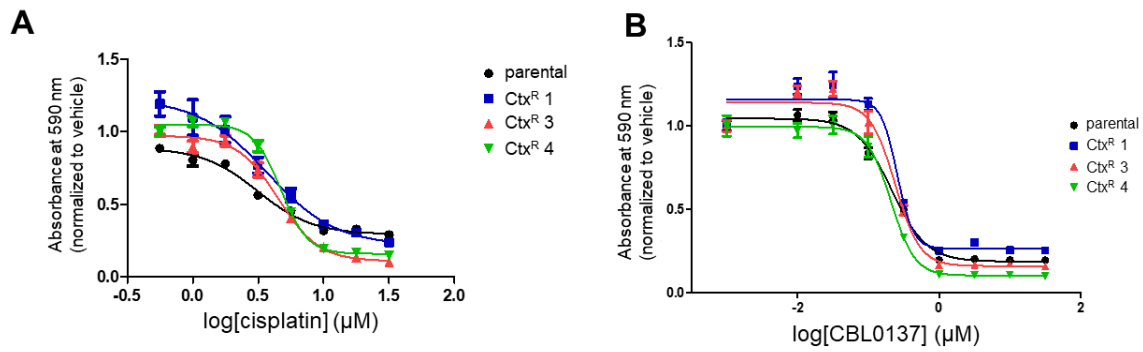


Figure 2.3. Cetuximab-resistant PE/CA-PJ49 cells are not resistant to cisplatin and CBL0137. A,B) Cisplatin (A) and CBL0137 (B) dose response assays in PE/CA-PJ49 parental and Ctx^R cells treated for 96 h, then stained with crystal violet. n=6.

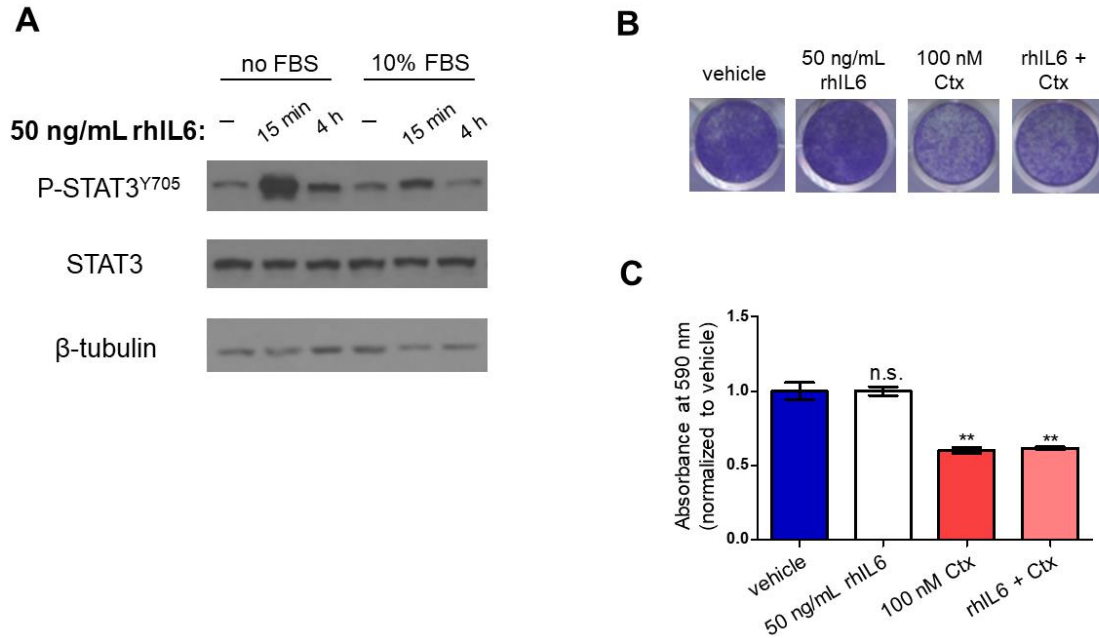


Figure 2.4. Addition of recombinant IL-6 does not promote cetuximab resistance in PE/CA-PJ49 parental cells. **A)** PE/CA-PJ49 parental cells were serum starved for 4 hours (no FBS) or remained in media containing 10% FBS (10% FBS), then treated with 50 ng/mL rhIL6 for 15 min or 4 hours. Cells were lysed in RIPA buffer and immunoblot was performed as described in Materials and Methods. β -tubulin image shown is from the STAT3 blot. **B)** PE/CA-PJ49 parental cells were treated for 96 h with vehicle (PBS), 50 ng/mL rhIL6, 100 nM Ctx, or the combination of Ctx and rhIL6, then stained with crystal violet. Images shown are representative of three biological replicates. **C)** Quantification of crystal violet staining in Fig. 2B. Student's two-tailed t-test was used to determine whether differences in absorbance at 590 nm were statistically significant (compared to vehicle-treated cells). $n=3$. ** $p<0.01$; n.s., not significant.

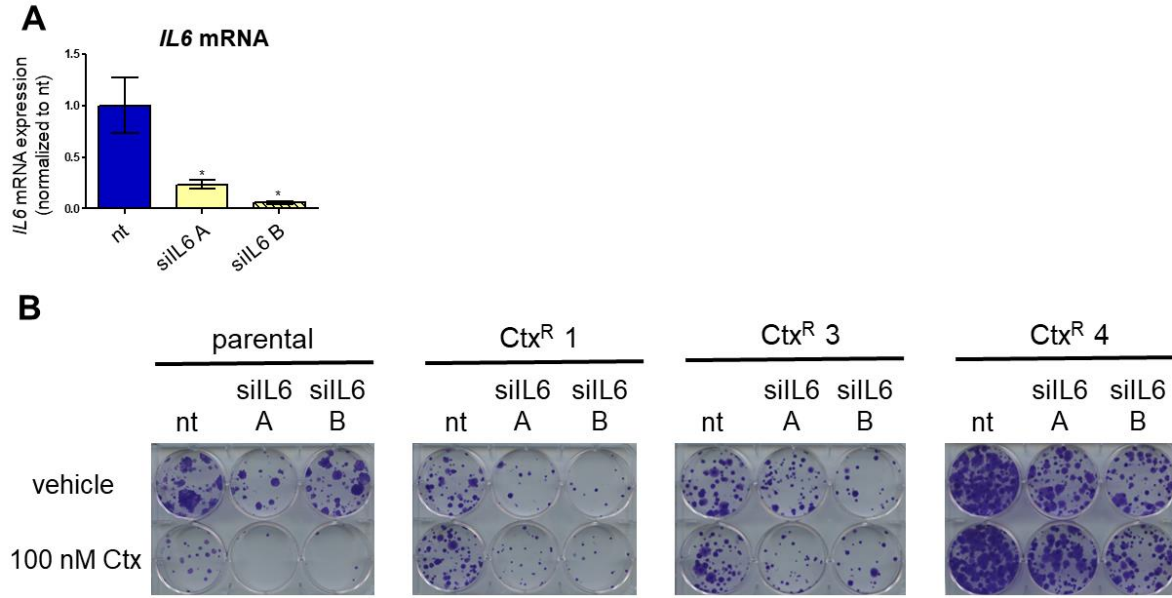


Figure 2.5. siRNA-mediated knockdown of *IL6* does not impact cetuximab response in PE/CA-PJ49 parental and Ctx^R cells. **A)** PE/CA-PJ49 parental cells were transfected with 10 nM nontargeting (nt) siRNA or one of two siRNAs targeting *IL6* (siL6 A and B). RNA was extracted 96 hours post-transfection and qPCR was conducted using the *IL6* primers listed in **Table 4.1** (normalized to *TBP*). n=3. *p<0.05. **B)** PE/CA-PJ49 parental and Ctx^R cells were plated at a low density and transfected with 10 nM siRNA the next day. On the following day, and every four days thereafter, the cells were treated with vehicle (PBS) or 100 nM Ctx. The cells were stained with crystal violet 13 days post-transfection.

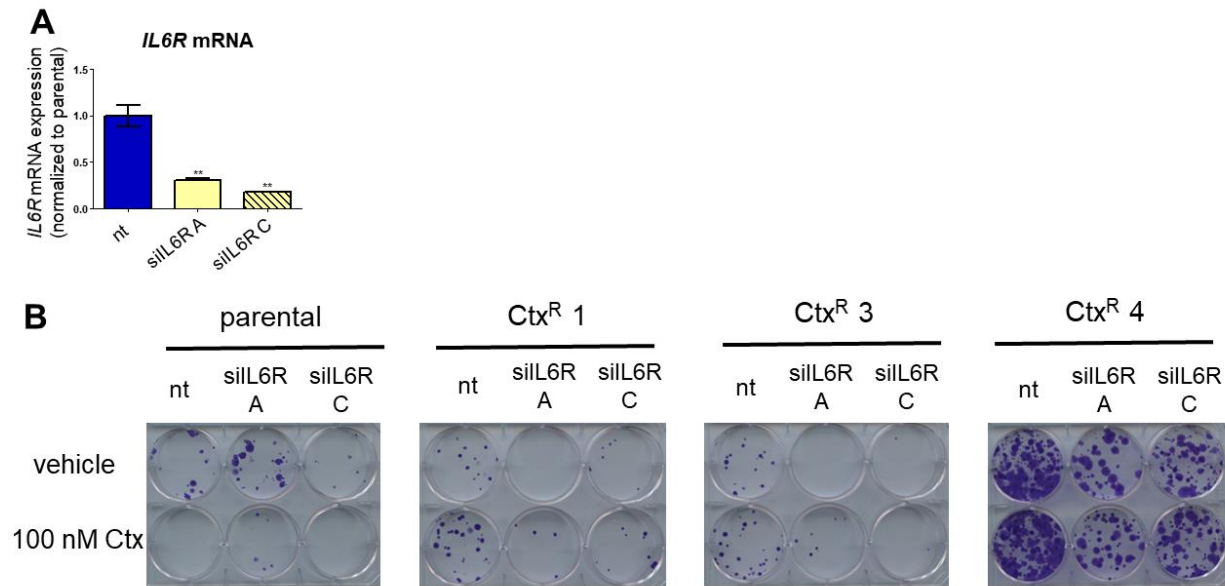


Figure 2.6. siRNA-mediated knockdown of *IL6R* does not impact cetuximab response in PE/CA-PJ49 parental and Ctx^R cells. **A)** PE/CA-PJ49 parental cells were transfected with 10 nM nontargeting (nt) siRNA or one of two siRNAs targeting *IL6R* (siL6R A and C). RNA was extracted 96 hours post-transfection and qPCR was conducted using the *IL6R* primers listed in **Table 4.1** (normalized to *TBP*). n=3. **p<0.01. **B)** PE/CA-PJ49 parental and Ctx^R cells were plated at a low density and transfected with 10 nM siRNA the next day. On the following day, and every four days thereafter, the cells were treated with vehicle (PBS) or 100 nM Ctx. The cells were stained with crystal violet 13 days post-transfection.

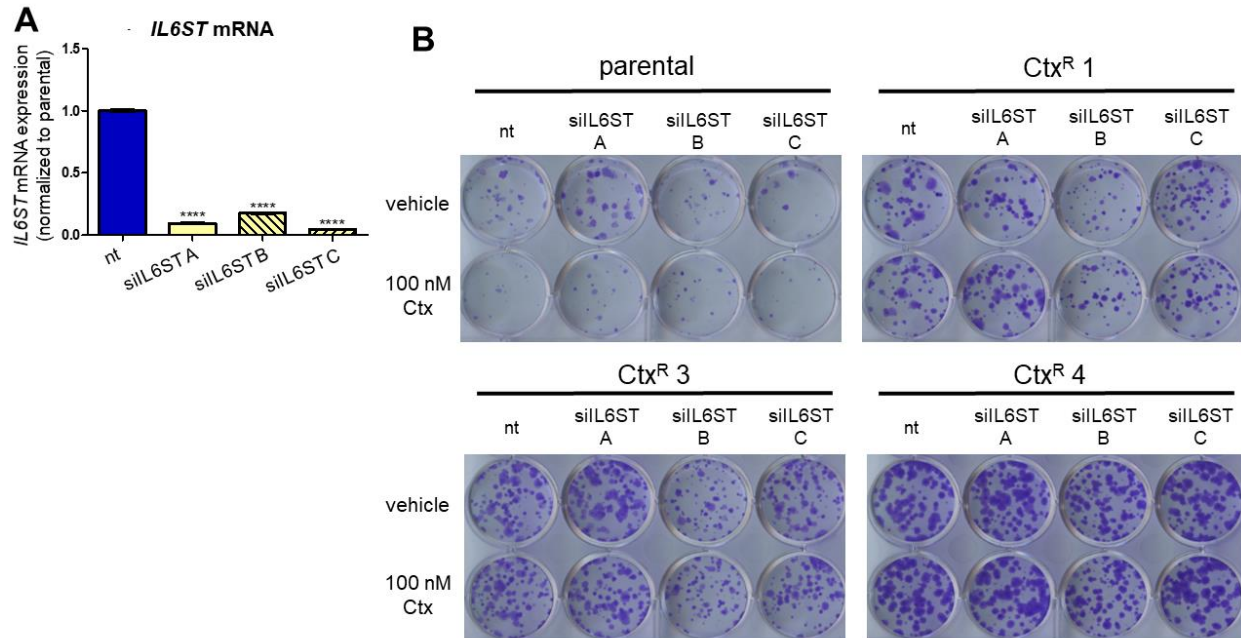


Figure 2.7. siRNA-mediated knockdown of *IL6ST* does not impact cetuximab response in PE/CA-PJ49 parental and Ctx^R cells. **A)** PE/CA-PJ49 parental cells were transfected with 10 nM nontargeting (nt) siRNA or one of three siRNAs targeting *IL6ST* (siL6ST A, B, and C). RNA was extracted 96 hours post-transfection and qPCR was conducted using the *IL6ST* primers listed in **Table 4.1** (normalized to *TBP*). n=3. ****p<0.0001. **B)** PE/CA-PJ49 parental and Ctx^R cells were plated at a low density and transfected with 10 nM siRNA the next day. On the following day, and every four days thereafter, the cells were treated with vehicle (PBS) or 100 nM Ctx. The cells were stained with crystal violet 13 days post-transfection.

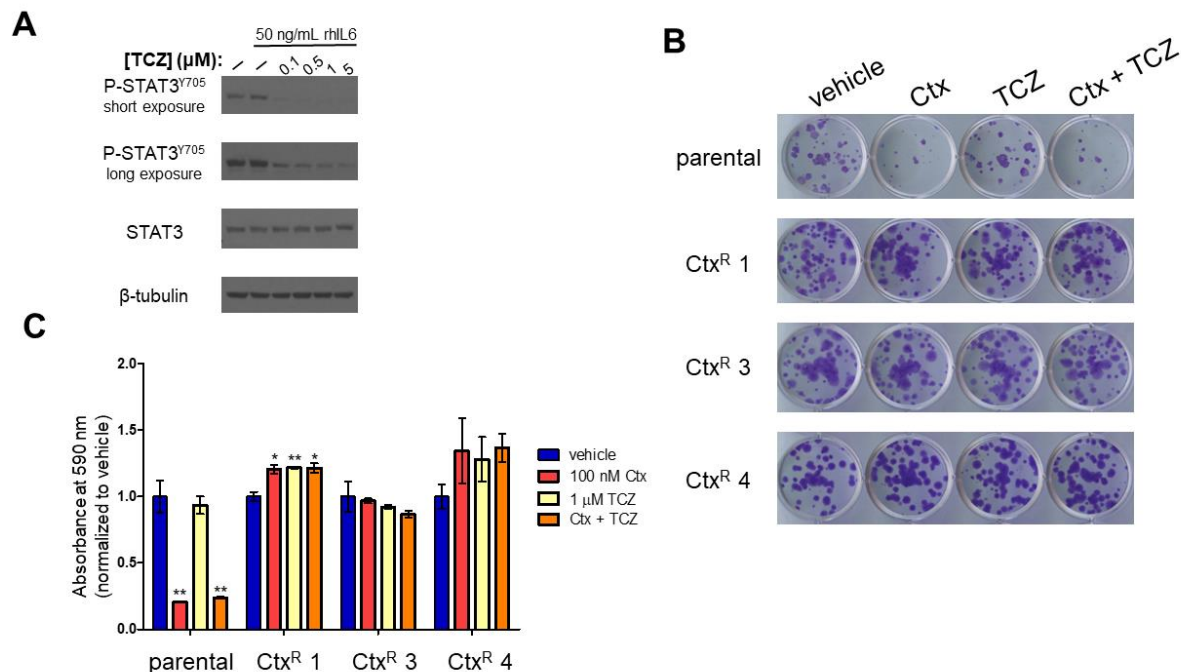


Figure 2.8. Pharmacological inhibition of the IL-6 pathway does not impact cetuximab response in PE/CA-PJ49 parental and Ctx^R cells. **A)** Serum-starved PE/CA-PJ49 parental cells were pre-treated for 2 hours with vehicle (PBS) or 100 nM – 5 μM TCZ, then treated with 50 ng/mL rhIL6 for 15 minutes. Cells were lysed in RIPA buffer and immunoblot was performed. β-tubulin image shown is from the STAT3 blot. **B)** PE/CA-PJ49 parental and Ctx^R cells were plated at a low density, then treated with vehicle (PBS), 100 nM Ctx, 1 μM TCZ, or the combination of Ctx and TCZ every 4 days. After a total of 12 days of treatment, the cells were stained with crystal violet. **C)** Crystal violet-stained cells from **(B)** were solubilized and absorbance at 590 nm was measured. Student's two-tailed t-test was used to determine whether differences in absorbance at 590 nm were statistically significant (compared to vehicle-treated cells). n=3. *p<0.05; **p<0.01.

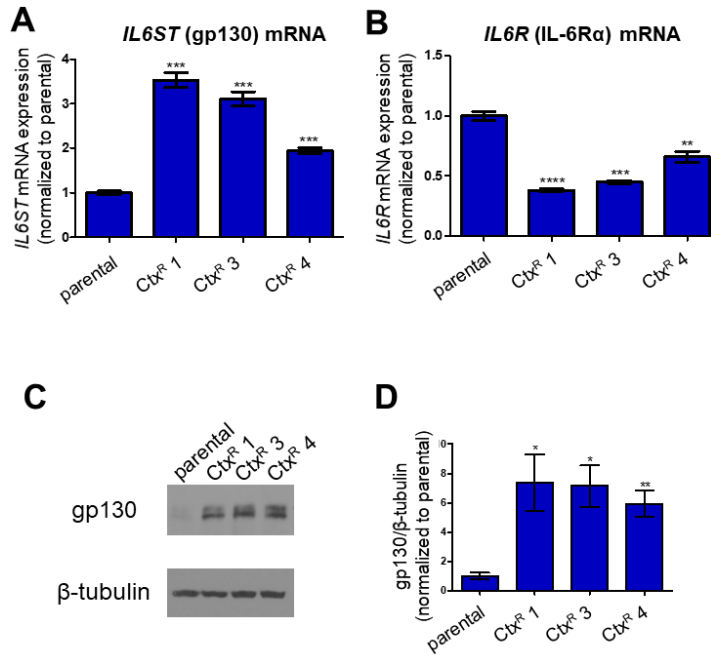


Figure 2.9. Expression of components of the IL-6 pathway are altered in HNSCC cells that have acquired resistance to cetuximab. **A,B)** RNA was extracted from PE/CA-PJ49 parental cells and cetuximab-resistant clones and qPCR was conducted using the *IL6ST* (**A**) or *IL6R* (**B**) primers listed in **Table 4.1** (normalized to *TBP*). n=3. **C)** Cells were lysed in RIPA buffer and immunoblot was performed. Images depicted are representative of three biological replicates. **D)** Densitometry was performed on the blots depicted in (**C**) using ImageJ as described in Materials and Methods. Densitometry values for gp130 were normalized to those for the loading control (β -tubulin). Student's t-test was used to determine whether differences in the gp130/ β -tubulin ratios in Ctx^R cells were statistically significant compared to parental cells. n=3. *p<0.05; **p<0.01; ***p<0.001; ****p<0.0001.

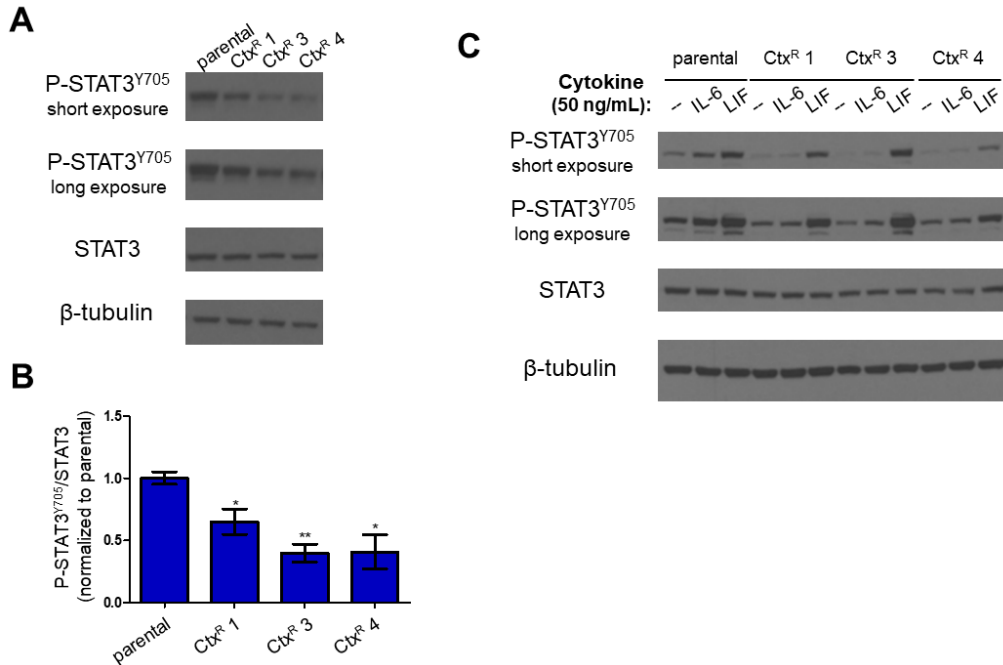


Figure 2.10. IL-6 signaling is impaired in PE/CA-PJ49 Ctx^R cells. **A)** PE/CA-PJ49 parental and Ctx^R cells were lysed in RIPA buffer and immunoblot was performed. Images shown are representative of three biological replicates. β-tubulin image shown is from the STAT3 blot. **B)** Densitometry was performed using ImageJ as described in Materials and Methods. Densitometry values for P-STAT3^{Y705} were normalized to those for total STAT3. Student's t-test was used to determine whether differences in the P-STAT3^{Y705}:STAT3 ratios in Ctx^R cells were statistically significant compared to parental cells. n=3. *p<0.05; **p<0.01. **C)** PE/CA-PJ49 parental and Ctx^R cells were serum starved for 4 hours, then treated for 15 minutes with 50 ng/mL rhIL6 or rhLIF. Cells were lysed in RIPA buffer and immunoblot was performed. β-tubulin image shown is from the P-STAT3^{Y705} blot.

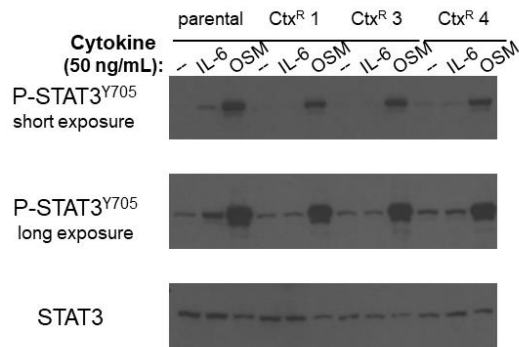


Figure 2.11. Phosphorylation of STAT3 is induced in PE/CA-PJ49 Ctx^R cells treated with rhOSM, but not rhIL6. PE/CA-PJ49 parental and Ctx^R cells were serum starved for 4 hours, then treated for 15 minutes with 50 ng/mL rhIL6 or rhOSM. Cells were lysed in RIPA buffer and immunoblot was performed.

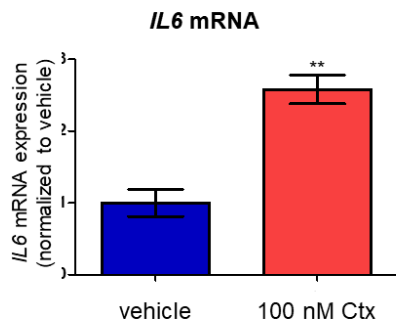


Figure 2.12. IL6 mRNA expression is increased in Ctx-treated PE/CA-PJ49 parental cells. PE/CA-PJ49 parental cells were treated with vehicle (PBS) or 100 nM Ctx. After 96 hours of treatment, RNA was extracted and qPCR was conducted using the *IL6* primers listed in **Table 4.1** (normalized to *TBP*). Student's two-tailed t-test was used to determine whether differences in IL6 expression were statistically significant. n=3. **p<0.01.

Chapter 3: Targeted sequencing analysis of cetuximab-sensitive and cetuximab-resistant variants of an HNSCC cell line

3.1 Introduction

Thus far, hypothesis-driven approaches to identify targetable mechanisms of resistance to cetuximab, including our own study on the role of IL-6 in cetuximab resistance, have not yielded any clinically validated therapeutic strategies to overcome cetuximab resistance in HNSCC. Alternative strategies may yield new insights into the biology of cetuximab resistance and expand the list of potential therapeutic targets in cetuximab-resistant HNSCC.

To glean more information from the cetuximab-resistant PE/CA-PJ49 cells, we used an unbiased approach, next-generation DNA sequencing using a targeted gene panel (UCSF500 Cancer Gene Panel) [91], to identify potential mediators of cetuximab resistance in these cells. In this panel, approximately 500 cancer-associated genes are sequenced, revealing single nucleotide variants (SNVs), insertions/deletions (indels), and copy number changes, as well as rearrangements that are commonly observed in cancer. This unbiased analysis could reveal novel genetic alterations correlated with acquired cetuximab resistance and inform future studies aimed at determining whether these alterations promote cetuximab resistance.

3.2 UCSF500 analysis in parental and cetuximab-resistant PE/CA-PJ49 cells

Genomic DNA isolated from the PE/CA-PJ49 parental and Ctx^R cells was sent to the UCSF Clinical Cancer Genomics Laboratory for sequencing. The data generated from the analysis were filtered as described in the Materials and Methods (Chapter 4) and used to compare the PE/CA-PJ49 parental and Ctx^R cells. Many of the SNVs and indels were shared

among the parental and Ctx^R cells (**Table 3.1**), providing further evidence (along with short tandem repeat analysis) that the Ctx^R cells are indeed PE/CA-PJ49 variants. The parental cells harbored more unique SNVs and indels than any of the three Ctx^R cell lines, but each cell line bore mutations that were not observed in the other three lines, suggesting heterogeneity among the clones (**Table 3.2**). Likewise, many of the copy number changes, including *TERT* and *PLAG1* amplifications, were shared among the cell lines (**Supplementary Table 1**).

Notably, the analysis did not uncover any alterations in *EGFR* in the parental or the Ctx^R cells, suggesting that alteration of the gene that encodes the protein targeted by cetuximab is not what mediates cetuximab resistance in these cells. In addition, although we observed increased gp130 levels in the Ctx^R cells, no alterations in the *IL6ST* gene were identified in the analysis (*IL6* and *IL6R* are not among the genes sequenced on this platform). A region on chromosome 17 that contains the *STAT3* gene appeared to be amplified in only the Ctx^R 1 and Ctx^R 4 in the filtered data, but reviewing the unfiltered data reveals that the parental and Ctx^R 3 cells also contain the chromosome 17 amplification, but with fold changes of 2 that fall below the cutoff of 2.5. This is in line with the observation that there is no increase in STAT3 protein expression in the Ctx^R cells compared to the parental cells (**Fig. 2.8**).

3.3 Unique mutations identified in cetuximab-resistant PE/CA-PJ49 cells

Targeted sequencing of our models identified a number of unique mutations in each of the four cell lines tested. The PE/CA-PJ49 parental cells contained more unique SNVs and indels than any of the Ctx^R cell lines, perhaps because each Ctx^R cell line was derived from a single clone of cetuximab-treated parental cells. However, each of the Ctx^R cells also harbored unique mutations. Their absence in the parental cells suggests that these mutations arose *de novo*

following the initiation of cetuximab treatment, but it remains possible that these mutations existed in the pool of PE/CA-PJ49 parental cells from which the Ctx^R cells were derived, but were not present in a sufficient fraction of the parental cells to be detectable in our targeted sequencing analysis. Notably, none of the mutations unique to the Ctx^R cells were shared among the three Ctx^R lines (**Table 3.2**).

Whether the unique mutations in the Ctx^R cells are simply correlated with or indeed promote cetuximab resistance remains unknown and will require additional experiments. However, given previously published information on the functions of the proteins encoded by these genes, we can speculate on the potential roles of these mutations in cetuximab resistance.

PE/CA-PJ49 Ctx^R 1

Both of the genes that were altered in only the PE/CA-PJ49 Ctx^R 1 cells, *KAT6A* and *NSDI* (**Table 3.2**), are involved in epigenetic regulation of gene expression.

KAT6A encodes lysine acetyltransferase 6A (KAT6A), a histone acetyltransferase [92,93]. The specific alteration identified in this analysis (p.1228_1228del) has not been reported; thus, its impact on KAT6A protein expression and function are unknown. However, the mutation occurs in the acidic domain of the protein, and nearby frameshift mutations affecting this region of the protein have been implicated as pathogenic variants in KAT6A syndrome, a rare neurodevelopmental disorder [93]. Notably, however, this mutation is a nonframeshift deletion, and may not have the deleterious effect that frameshift mutations in this region have. On the other hand, *KAT6A* mRNA levels are increased in glioblastoma samples compared to normal brain tissue, and KAT6A has been shown to promote glioma cell proliferation via upregulation of *PIK3CA* expression and subsequent activation of PI3K/Akt signaling [92]. Thus,

if the mutation identified in the Ctx^R 1 cells is an activating mutation, this *KAT6A* alteration could promote cetuximab resistance by activating PI3K/Akt signaling, a previously identified mediator of cetuximab resistance [5,18,52,60].

NSDI encodes nuclear receptor binding SET domain protein 1 (NSD1), a histone methyltransferase [2,10,94]. The *NSDI* mutation identified in the Ctx^R 1 cells, p.G1132fs, has not been previously reported. However, novel inactivating mutations in *NSDI* were identified in 29 of the 279 HNSCC tumors in the TCGA published in 2015 (all in HPV-negative tumors) [10], and the constellation of non-hotspot mutations suggest that this mutation, too, may be inactivating, potentially resulting in DNA hypomethylation. *NSDI* inhibition has been shown to enhance sensitivity to cisplatin and carboplatin in head and neck cancer cell lines [2,94], but the impact of loss-of-function mutations in *NSDI* on cetuximab response is unknown. Notably, alterations in DNA methylation patterns have been associated with acquired resistance to cetuximab [95]. This will be discussed more in Section 3.4.

PE/CA-PJ49 Ctx^R 3

PE/CA-PJ49 Ctx^R 3 cells, but not the other PE/CA-PJ49 clones analyzed, contain a nonsynonymous mutation (p.D774E) in *CHD5*, the gene encoding the tumor suppressor chromodomain helicase DNA binding protein 5 (CHD5) [96] and a frameshift substitution (c.864delinsCC) in *HNF1A*, which encodes hepatocyte nuclear factor 1 alpha, a transcription factor that is infrequently mutated (~1%) in HNSCC [10,97,98]. The functional significance of these mutations, and whether they play a role in cetuximab resistance in the Ctx^R 3 cells, is unknown.

PE/CA-PJ49 Ctx^R 4

EIF1AX, one of the five genes that is mutated in only the Ctx^R 4 cells (**Table 3.2**), encodes eukaryotic translation initiation factor 1A, X-linked, a component of the translation preinitiation complex [99,100]. This gene is rarely altered (~2%) in HNSCC, and the majority of the alterations are deep deletions [10,97,98]. However, in papillary thyroid cancer, the majority of the alterations are mutations [97–99]. Though these mutations are uncommon (1.21% of the 496 cases included in the TCGA analysis), it was suggested that *EIF1AX* could be an oncogenic driver in papillary thyroid cancer (PTC) due to its near-mutual exclusivity with *KRAS* and *BRAF* mutations and its high rate of alteration (48%) in uveal melanomas with disomy 3 [99,101]. *EIF1AX* mutations were also identified, this time co-occurring with *RAS* mutations, in poorly differentiated thyroid cancers (PDTC) and anaplastic thyroid cancers (ATC) [100]. However, these mutations occur near the N-terminus of the protein in both PTC and uveal melanoma [99,101], and at a hotspot splice acceptor site (A113splice) in PDTC and ATC [100], whereas the mutation identified in the Ctx^R 4 cells (p.K56N) occurs at a different location; thus, the functional significance of this mutation is unknown.

PIK3R2 encodes p85 β , a regulatory subunit of PI3K that is rarely mutated in HNSCC (~1%) [10,97,98,102]. The functional significance of the non-frameshift substitution (c.700_702CGT) identified in the Ctx^R 4 cells is unknown; however, in a study focusing on mutations in *PIK3R2* and other PI3K pathway-associated genes in endometrial cancer, it was suggested that *PIK3R2* mutations may phenocopy loss of the tumor suppressor phosphatase and tensin homolog (PTEN) [102], an alteration that leads to aberrant hyperactivation of PI3K/Akt signaling.

The presence of a stopgain mutation (p.W563*) in *RBI* (which encodes retinoblastoma protein) suggests that this tumor suppressor may be functionally inactivated in the Ctx^R 4 cells. As the CDK4/6 inhibitor palbociclib was recently shown to act synergistically with either lapatinib or afatinib (tyrosine kinase inhibitors that target EGFR and HER2) to inhibit proliferation in HNSCC cell lines [103], it may be worthwhile to test whether co-treatment of the Ctx^R 4 cells with palbociclib has an impact on their response to cetuximab.

3.4 Conclusions and future directions

As we demonstrated in Chapter 2, alterations that are correlated with cetuximab resistance do not necessarily confer resistance to cetuximab (**Fig. 2.4**); thus, the unique mutations identified in the Ctx^R cells may not play a role in acquired cetuximab resistance. Nonetheless, unbiased analyses such as these may uncover novel candidate biomarkers and/or therapeutic targets that can then be validated in subsequent functional studies. A reasonable next step to follow the UCSF500 analysis would be to determine whether the mutations identified in the Ctx^R cells promote cetuximab resistance by expressing these mutations in cetuximab-sensitive cells, or eliminating the mutations from the Ctx^R cells, and determining whether these interventions impact cetuximab response.

In light of a recent publication focusing on the timing of alterations developed during the acquisition of cetuximab resistance in an HNSCC cell line [95], the mutations in genes associated with epigenetic regulation, such as *NSDI*, identified in the targeted sequencing analysis may be of particular interest. In the aforementioned study, published by Stein-O'Brien and colleagues, a rigorous time course analysis consisting of weekly collection of samples for RNA-sequencing and DNA methylation analyses revealed that, while transcriptional changes

arose quickly following initiation of cetuximab treatment, stable alterations in DNA methylation were observed only after resistance was established, highlighting a difference between adaptive responses to treatment and acquired resistance. In addition, we recently reported that the chromatin reader protein BRD4 promotes cetuximab resistance in HNSCC cell line models, including the PE/CA-PJ49 Ctx^R cells used in this study [56]. Studying epigenetic alterations in cetuximab-resistant cells, whether or not these alterations are related to the mutations detected in our targeted sequencing analysis, may identify additional mechanisms of cetuximab resistance and potential candidates to target to prevent and/or overcome cetuximab resistance.

3.5 Tables

Table 3.1. SNVs and indels identified in all PE/CA-PJ49 parental and Ctx^R cell lines.

ARID1A p.A54S	NOTCH1 p.P1730L
ARID1A p.F1457S	NOTCH1 p.R365C
BRCA2 p.I247V	PAK1 p.E74D
CDKN2A p.M52fs	PEX11B p.G62V
CLPTM1L p.316_317del	PRDM1 p.R192C
COL1A1 p.P823A	PTPRD p.I1821V
CREBBP p.S1761*	RASA1 c.829_840GTAGAAGATAGA
FANCG c.176-2A>G	RASA1 p.A804fs
FAT1 c.11049_11050TT	RASA1 p.D280delinsDR
FLCN p.A90S	RASA2 p.Q286*
IPMK p.S261P	SYNE1 p.R4152C
JAK3 p.L1047V	TERT promoter
KMT2D p.M1478fs	TSC2 p.R1268C
† MIR4457 promoter	† ZFHX p.1823_1823del

Exceptions (†) were observed in only the parental and Ctx^R 3 cells. Abbreviations: del, deletion; fs, frameshift mutation.

Table 3.2. SNVs and indels unique to individual cell lines.

Parental	Ctx ^R 1	Ctx ^R 3	Ctx ^R 4
<ul style="list-style-type: none"> • CHD1 p.K347R • CHD5 p.101_102del • EMSY p.E74K • GNAQ p.V340F • MTOR p.R2443Q • MYH9 p.D1293N • MYH9 p.E1270K • NFKBIA p.E40K • PDGFRA p.Y136fs • PLCB4 	<ul style="list-style-type: none"> • KAT6A p.1228_1228del • NSD1 p.G1132fs 	<ul style="list-style-type: none"> • CHD5 p.D774E • HNF1A c.864delinsCC 	<ul style="list-style-type: none"> • EIF1AX p.K56N • PIK3R2 c.700_702CGT • PRKDC exonic UNKNOWN • RB1 p.W563* • ZFHX4 p.2007_2007del

Abbreviations: del, deletion; delins, deletion-insertion; fs, frameshift mutation.

Chapter 4: Materials and Methods

Cell culture

Cell lines were maintained in Dulbecco's Modified Eagle's Medium (DMEM; Corning 10-013-CM) containing 10% fetal bovine serum (FBS; Gemini Bio-Products #900-108) and penicillin/streptomycin (Gibco 15140-122). PE/CA-PJ49 cells were purchased from Sigma-Aldrich. Cell lines were authenticated by short tandem repeat (STR) analysis performed by the University of California, Berkeley DNA Sequencing Facility at least once every 6 months.

Generation of cetuximab-resistant cell lines

We previously reported generation of the PE/CA-PJ49 cell line models of acquired cetuximab resistance [56]. STR analysis was performed on the cetuximab-resistant cell lines to confirm that the profiles matched those of the parental cell line.

Dose-response assays

Cells were plated in 96-well plates and incubated overnight. The next day, the media was replaced with media containing the indicated concentrations of drug or an equivalent volume of vehicle. After 96 hours of treatment, cells were rinsed with ice-cold phosphate-buffered saline (PBS) and stained with crystal violet solution (0.5% crystal violet [Sigma C0775] in 25% methanol). To quantify results, crystal violet-stained cells were solubilized in a 1:1 mixture of 200 mM sodium citrate and 100% ethanol and absorbance at 590 nm was read using a Biotek Epoch Microplate Spectrophotometer. Erlotinib (S1023), afatinib (S7810), and lapatinib (S2111) were purchased from Selleckchem. Cisplatin was purchased from the University of Pittsburgh

Cancer Institute Pharmacy. CBL0137 was provided by Dr. George Stark and Dr. Sarmishtha De (Cleveland Clinic).

Gene expression analysis

RNA was isolated from HNSCC cells using the RNeasy Mini Kit (Qiagen, 74106), according to the manufacturer's protocol (excluding the optional DNase digestion step) and eluted in nuclease-free water (Fisher BioReagents, BP2484-50). RNA concentration and purity (OD 260/280) were determined using the Biotek Epoch Microplate Spectrophotometer. One microgram of RNA per sample was converted to complementary DNA (cDNA) in an Eppendorf PCR machine using either iScript™ Reverse Transcription Supermix for RT-qPCR (Bio-Rad, #1708840) or iScript™ cDNA Synthesis Kit (Bio-Rad, #1708890), according to the manufacturer's instructions. Quantitative reverse transcription PCR (qRT-PCR) was performed in the CFX96 Touch™ Real-Time PCR Detection System (Bio-Rad) using the iTaq™ Universal SYBR® Green Supermix (Bio-Rad, #1725124) according to the manufacturer's instructions. Assay of each sample was performed in technical duplicate. The sequences of the primers used are listed in **Table 3.1**. The delta-delta Ct method was used to determine relative mRNA expression (normalized to the reference gene TATA-box-binding protein [*TBP*]). GraphPad Prism was used to conduct Student's two-tailed t-test to determine whether changes between experimental conditions were statistically significant. Controls for each experiment and number of biological replicates are indicated in the respective figure legends.

Table 4.1. qPCR primers.

Primer Name	Sequence
<i>IL6</i> forward	GGTACATCCTCGACGGCATCT
<i>IL6</i> reverse	GTGCCTCTTTGCTGCTTTCAC
<i>IL6R</i> forward	AGTGTCGGGAGCAAGTTCAG
<i>IL6R</i> reverse	GGCTGCAAGATTCCACAACC
<i>IL6ST</i> forward	AGGACCAAAGATGCCTCAAC
<i>IL6ST</i> reverse	GAATGAAGATCGGGTGGATG
<i>TBP</i> forward	CCCATGACTCCCATGACC
<i>TBP</i> reverse	TTTACAACCAAGATTCCTGTGG

Immunoblot analysis

Cells for immunoblot analysis were rinsed twice with ice-cold PBS and lysed on ice in radioimmunoprecipitation assay (RIPA) buffer (150 mM sodium chloride, 5 mM EDTA pH 8.0, 50 mM Tris pH 8.0, 1% NP-40 Surfact-Amps Detergent Solution, 0.5% sodium deoxycholate, 0.1% sodium dodecyl sulfate [SDS]) supplemented with cOmplete Protease Inhibitor Cocktail (Roche 11836145001) and PhosSTOP Phosphatase Inhibitor Cocktail Tablets (Roche 04 906 837 001). Cells undergoing lysis were briefly vortexed, then centrifuged for 10 minutes at 13,200 RCF at 4°C. Supernatants were transferred to fresh 1.7-mL microcentrifuge tubes and protein concentrations were determined using Protein Assay Dye Reagent (Bio-Rad #5000006). Lysates were mixed with the appropriate volume of 4X sample buffer (230 mM Tris-HCl pH 6.8, 7% SDS, 32% glycerol, 0.1% w/v bromophenol blue, 9% β-mercaptoethanol), boiled for 5 minutes, electrophoresed on 10% polyacrylamide Tris-glycine gels, and transferred to Immun-Blot PVDF membranes (Bio-Rad #1620177) on a Trans-Blot SD Semi-Dry Transfer Cell (Bio-Rad). Membranes were then blocked in 5% nonfat dry milk (Apex 20-241) in Tris-buffered saline with Tween 20 (TBST) and probed overnight at 4°C with primary antibodies diluted in 2.5% bovine serum albumin (BSA; Sigma A3912) in TBST. Primary antibodies used in this study were purchased from Cell Signaling Technology (P-STAT3^{Y705} [#9145, rabbit monoclonal] and

STAT3 [#4904, rabbit monoclonal]), Santa Cruz Biotechnology (gp130 [sc-376280, Lot #B1717, mouse monoclonal]), and Abcam (β -tubulin [ab6046, rabbit polyclonal]).

The next day, membranes were washed 5-6 times in TBST, blocked for 15-30 min in 5% nonfat dry milk in TBST, and incubated in the appropriate horseradish peroxidase (HRP)-conjugated secondary antibody for 45-90 min at room temperature. Secondary antibodies used in this study were purchased from Bio-Rad (Goat Anti-Rabbit IgG (H+L)-HRP Conjugate [#1706515] and Goat Anti-Mouse IgG (H+L)-HRP Conjugate [#1706516]). After incubation in secondary antibody, membranes were washed 5-6 times in TBST and incubated in the chemiluminescent HRP substrate Western Blotting Luminol Reagent (Santa Cruz Biotechnology, sc-2048) according to the manufacturer's instructions. Films (GeneMate F-9024-8X10) were scanned at 300 dpi and images were converted to greyscale prior to densitometric analysis using ImageJ (National Institutes of Health), but were not otherwise altered. Density values for the proteins of interest were divided by those of the total protein (for phosphorylated proteins) or the loading control (β -tubulin) (for all other proteins) from the corresponding lane of the same membrane. Data were normalized by dividing the values for each sample by the average of those for the control samples (controls for each experiment and number of biological replicates are indicated in the respective figure legends). GraphPad Prism was used to conduct Student's two-tailed t-test to determine whether changes between experimental conditions were statistically significant.

Enzyme-linked immunosorbent assay (ELISA)

Cells were plated at 50,000 cells per well in 24-well culture plates in DMEM supplemented with 10% FBS and penicillin/streptomycin and allowed to attach overnight. The next day, cells were

gently rinsed with sterile PBS and media was replaced with 500 μ L DMEM (without FBS or penicillin/streptomycin). After 72 hours of incubation, conditioned media were removed and centrifuged for 10 min at 10,000 RCF at 4°C. Supernatants were transferred to fresh 1.7-mL microcentrifuge tubes and frozen at -80°C for subsequent analysis. The concentration of IL-6 in the cell culture supernatants was determined using the Human IL-6 DuoSet ELISA kit (R&D Systems DY206) according to the manufacturer's instructions. Plates were read at 450 nm on the Biotek Epoch Microplate Spectrophotometer, with wavelength correction at 540 nm. Assays were performed in technical duplicate. The number of biological replicates is indicated in the respective figure legends. GraphPad Prism was used to conduct Student's two-tailed t-test to determine whether changes in concentration of secreted IL-6 were statistically significant between parental PE/CA-PJ49 cells and PE/CA-PJ49 cells that had acquired resistance to cetuximab.

Cytokines

Recombinant cytokines used in this study were purchased from PeproTech (Recombinant Human IL-6 [200-06], Recombinant Human LIF [300-05], and Recombinant Human Oncostatin M (209 a.a.) [300-10T]). Lyophilized cytokines were reconstituted in sterile nuclease-free water (Fisher BioReagents, BP2484-50) before use.

siRNA transfection

Cells were plated in DMEM containing 10% FBS and penicillin/streptomycin and allowed to attach overnight. The next day, immediately prior to transfection, media was replaced with DMEM supplemented with 10% FBS (without antibiotics). A final concentration of 10 nM

siRNA (control [nontargeting] siRNA or one of at least two distinct siRNA sequences per target) was transfected into cells using Lipofectamine™ RNAiMAX Transfection Reagent (ThermoFisher Scientific, #13778500) according to the manufacturer's instructions, using 5 µL RNAiMAX in a total volume of 1.5 mL for 6-well plates and 2.5 µL RNAiMAX in a total volume of 750 µL for 12-well plates. The siRNA-containing media was replaced with DMEM supplemented with 10% FBS and penicillin/streptomycin 4 hours post-transfection. Knockdown was validated using qPCR. All siRNAs were purchased from Origene (IL6 Human siRNA Oligo Duplex [SR302379], IL6R Human siRNA Oligo Duplex [SR302380], and IL6ST Human siRNA Oligo Duplex [SR302381]).

Clonogenic survival assays

Cells were plated at 250 cells per well in 12-well cell culture plates. The next day, cells were treated as indicated for the particular experiment. Media containing vehicle and/or drug was replaced every four days. After 12 days of treatment, cells were stained with crystal violet solution (0.5% crystal violet [Sigma C0775] in 25% methanol).

UCSF500 Cancer Gene Panel

Genomic DNA was extracted from the PE/CA-PJ49 parental and Ctx^R cells using the Qiagen DNeasy Blood & Tissue kit (Catalog number 69504) according to the manufacturer's instructions, then submitted to the UCSF Clinical Cancer Genomics Laboratory for testing using the UCSF500 Cancer Gene Panel. The UCSF 500 Cancer Gene Panel uses capture-based next-generation sequencing to target and analyze the coding regions (exons) of 479 cancer genes, as well as select introns of 47 genes. Target enrichment was performed by hybrid capture using

custom oligonucleotides (Roche Nimblegen). Sequencing of captured libraries was performed on an Illumina HiSeq 2500 in rapid run mode (2 X 101 bp read length). Sequence reads were de-duplicated to allow for accurate allele frequency determination and copy number calling. The analysis used open source or licensed software for alignment to the human reference sequence UCSC build hg19 (NCBI build 37) and variant calling. Common germline polymorphisms were eliminated from analysis using the complete list of germline variants from dbSNP. Rare variants were reviewed by using a filtering threshold of 0.1% in large population databases (gnomAD; <https://gnomad.broadinstitute.org/>). Additional filtering to eliminate technology specific sequencing artifacts was performed before analyzing the data.

References

1. Leemans CR, Braakhuis BJM, Brakenhoff RH. The molecular biology of head and neck cancer. *Nat Rev Cancer*. 2011;11(1):9–22.
2. Bui N, Huang JK, Bojorquez-gomez A, Licon K, Sanchez KS, Tang SN, et al. Disruption of NSD1 in Head and Neck Cancer Promotes Favorable Chemotherapeutic Responses Linked to Hypomethylation. *Mol Cancer Ther*. 2018;17(7):1585–95.
3. Cohen EEW, Bell RB, Bifulco CB, Burtness B, Gillison ML, Harrington KJ, et al. The Society for Immunotherapy of Cancer consensus statement on immunotherapy for the treatment of squamous cell carcinoma of the head and neck (HNSCC). *J Immunother Cancer*. 2019;7(1):184.
4. Behren A, Kamenisch Y, Muehlen S, Flechtenmacher C, Haberkorn U, Hilber H, et al. Development of an oral cancer recurrence mouse model after surgical resection. *Int J Oncol*. 2010;36:849–55.
5. Cassell A, Freilino ML, Lee J, Barr S, Wang L, Panahandeh MC, et al. Targeting TORC1/2 enhances sensitivity to EGFR inhibitors in head and neck cancer preclinical models. *Neoplasia*. 2012;14(11):1005–14.
6. Pollock NI, Grandis JR. HER2 as a therapeutic target in head and neck squamous cell carcinoma. *Clin Cancer Res*. 2014;21(3):526–33.
7. Johnston PA, Sen M, Hua Y, Camarco DP, Shun TY, Lazo JS, et al. HCS campaign to identify selective inhibitors of IL-6-induced STAT3 pathway activation in head and neck cancer cell lines. *Assay Drug Dev Technol*. 2015;13(7):356–76.
8. Kobayashi K, Hisamatsu K, Suzui N, Hara A, Tomita H, Miyazaki T. A Review of HPV-Related Head and Neck Cancer. *J Clin Med*. 2018;1–11.

9. Fakhry C, Westra WH, Li S, Cmelak A, Ridge JA, Pinto H, et al. Improved Survival of Patients With Human Papillomavirus – Positive Head and Neck Squamous Cell Carcinoma in a Prospective Clinical Trial. 2008;261–9.
10. Lawrence MS, Sougnez C, Lichtenstein L, Cibulskis K, Lander E, Gabriel SB, et al. Comprehensive genomic characterization of head and neck squamous cell carcinomas. *Nature*. 2015;517(7536):576–82.
11. Vermorken JB, Mesia R, Rivera F, Remenar E, Kawecki A, Rottey S, et al. Platinum-Based Chemotherapy plus Cetuximab in Head and Neck Cancer. *N Engl J Med*. 2008;359(11):1116–27.
12. Mehra R, Cohen RB, Burtneess B a. The role of cetuximab for the treatment of squamous cell carcinoma of the head and neck. *Clin Adv Hematol Oncol*. 2008;6(10):742–50.
13. Bonner JA, Harari PM, Giralt J, Azarnia N, Shin DM, Cohen RB, et al. Radiotherapy plus Cetuximab for Squamous- Cell Carcinoma of the Head and Neck. *New Engl Jounal Med*. 2006;354(6):567–78.
14. Cassell A, Grandis JR. Investigational EGFR-targeted therapy in head and neck squamous cell carcinoma. *Expert Opin Investig Drugs*. 2010;19(6):709–22.
15. Luedke E, Jaime-Ramirez AC, Bhave N, Roda J, Choudhary MM, Kumar B, et al. Cetuximab therapy in head and neck cancer: Immune modulation with interleukin-12 and other natural killer cell-activating cytokines. *Surgery*. 2012;152(3):431–40.
16. Li H, Wawrose JS, Gooding WE, Garraway LA, Yan VW, Peyser ND, et al. Genomic analysis of head and neck squamous cell carcinoma cell lines and human tumors: A rational approach to preclinical model selection. *Mol Cancer Res*. 2014;12(4):571–82.
17. Chen CC, Chen WC, Lu CH, Wang WH, Lin PY, Lee K Der, et al. Significance of

- interleukin-6 signaling in the resistance of pharyngeal cancer to irradiation and the epidermal growth factor receptor inhibitor. *Int J Radiat Oncol Biol Phys*. 2010;76(4):1214–24.
18. Rebucci M, Peixoto P, Dewitte A, Wattez N, de Nuncques M-A, Rezvoy N, et al. Mechanisms underlying resistance to cetuximab in the HNSCC cell line: Role of AKT inhibition in bypassing this resistance. *Int J Oncol*. 2011;38:189–200.
 19. Genova C, Hirsch FR. Clinical potential of necitumumab in non-small cell lung carcinoma. *Onco Targets Ther*. 2016;9:5427–37.
 20. Iqbal N, Iqbal N. Human Epidermal Growth Factor Receptor 2 (HER2) in Cancers: Overexpression and Therapeutic Implications. *Mol Biol Int*. 2014;2014.
 21. Moasser MM. The Oncogene HER2: Its Signaling and Transforming Functions and Its Role in Human Cancer Pathogenesis. *Oncogene*. 2007;26(45):6469–87.
 22. Boulbes DR, Arold ST, Chauhan GB, Blachno K V., Deng N, Chang WC, et al. HER family kinase domain mutations promote tumor progression and can predict response to treatment in human breast cancer. *Mol Oncol*. 2015;9(3):586–600.
 23. Vouri M, Croucher DR, Kennedy SP, An Q, Pilkington GJ, Hafizi S. Axl-EGFR receptor tyrosine kinase hetero-interaction provides EGFR with access to pro-invasive signalling in cancer cells. *Oncogenesis*. 2016;5(10):e266.
 24. Prabhakar CN. Epidermal growth factor receptor in non-small cell lung cancer. *Transl lung cancer Res*. 2015;4(2):110–8.
 25. Sharafinski ME, Ferris RL, Ferrone S, Grandis JR. Epidermal growth factor receptor targeted therapy of squamous cell carcinoma of the head and neck. *Head Neck*. 2010;32(10):1412–21.

26. Hocking CM, Price TJ. Panitumumab in the management of patients with KRAS wild-type metastatic colorectal cancer. *Therap Adv Gastroenterol*. 2014;7(1):20–37.
27. Hsu H-C, Thiam TK, Lu Y-J, Yeh CY, Tsai W-S, You JF, et al. Mutations of KRAS/NRAS/BRAF predict cetuximab resistance in metastatic colorectal cancer patients. *Oncotarget*. 2016;7(16):22257–70.
28. Gao J, Ulekleiv CH, Halstensen TS. Epidermal growth factor (EGF) receptor-ligand based molecular staging predicts prognosis in head and neck squamous cell carcinoma partly due to deregulated EGF- induced amphiregulin expression. *J Exp Clin Cancer Res*. 2016;35(1):151.
29. Carcereny E, Morán T, Capdevila L, Cros S, Vilà L, de Los Llanos Gil M, et al. The epidermal growth factor receptor (EGFR) in lung cancer. *Transl Respir Med*. 2015;3:1.
30. Bhargava R, Gerald WL, Li AR, Pan Q, Lal P, Ladanyi M, et al. EGFR gene amplification in breast cancer: correlation with epidermal growth factor receptor mRNA and protein expression and HER-2 status and absence of EGFR-activating mutations. *Mod Pathol*. 2005;18(8):1027–33.
31. Vivanco I, Ian Robins H, Rohle D, Campos C, Grommes C, Nghiemphu PL, et al. Differential sensitivity of glioma- versus lung cancer-specific EGFR mutations to EGFR kinase inhibitors. *Cancer Discov*. 2012;2(5):458–71.
32. Soung YH, Lee JW, Kim SY, Wang YP, Jo KH, Moon SW, et al. Somatic mutations of the ERBB4 kinase domain in human cancers. *Int J Cancer*. 2006;118(6):1426–9.
33. Li AR, Chitale D, Riely GJ, Pao W, Miller VA, Zakowski MF, et al. EGFR Mutations in Lung Adenocarcinomas. *J Mol Diagnostics*. 2008;10(3):242–8.
34. Konduri K, Gallant J-N, Chae YK, Giles FJ, Gitlitz BJ, Gowen K, et al. EGFR Fusions as

- Novel Therapeutic Targets in Lung Cancer. *Cancer Discov.* 2016;6(6):601–11.
35. Jaiswal BS, Kljavin NM, Stawiski EW, Chan E, Parikh C, Durinck S, et al. Oncogenic ERBB3 Mutations in Human Cancers. *Cancer Cell.* 2013;23(5):603–17.
 36. Quesnelle KM, Wheeler SE, Ratay MK, Grandis JR. Preclinical modeling of EGFR inhibitor resistance in head and neck cancer. *Cancer Biol Ther.* 2012;13(10):935–45.
 37. Tan AR, Moore DF, Hidalgo M, Doroshow JH, Poplin E a., Goodin S, et al. Pharmacokinetics of cetuximab after administration of escalating single dosing and weekly fixed dosing in patients with solid tumors. *Clin Cancer Res.* 2006;12(21):6517–22.
 38. Chen LF, Cohen EEW, Grandis JR. New strategies in head and neck cancer: understanding resistance to epidermal growth factor receptor inhibitors. *Clin Cancer Res.* 2010;16(9):2489–95.
 39. Martinelli E, De Palma R, Orditura M, De Vita F, Ciardiello F. Anti-epidermal growth factor receptor monoclonal antibodies in cancer therapy. *Clin Exp Immunol.* 2009;158(1):1–9.
 40. Bou-Assaly W, Mukherji S. Cetuximab (Erbix). *Am J Neuroradiol.* 2010;31(4):626–7.
 41. James AM, Cohen AD, Campbell KS. Combination immune therapies to enhance anti-tumor responses by NK cells. *Front Immunol.* 2013;4(DEC):1–12.
 42. Klöss S, Chambron N, Gardlowski T, Weil S, Koch J, Esser R, et al. Cetuximab reconstitutes pro-inflammatory cytokine secretions and tumor-infiltrating capabilities of sMICA-inhibited NK cells in HNSCC tumor spheroids. *Front Immunol.* 2015;6(NOV):1–18.
 43. Vermorken JB, Trigo J, Hitt R, Koralewski P, Diaz-Rubio E, Rolland F, et al. Open-label, uncontrolled, multicenter Phase II study to evaluate the efficacy and toxicity of cetuximab

- as a single agent in patients with recurrent and/or metastatic squamous cell carcinoma of the head and neck who failed to respond to platinum-based the. *J Clin Oncol*. 2007;25(16):2171–7.
44. Martins RG, Parvathaneni U, Bauman JE, Sharma AK, Raez LE, Papagikos MA, et al. Cisplatin and radiotherapy with or without erlotinib in locally advanced squamous cell carcinoma of the head and neck: A randomized phase ii trial. *J Clin Oncol*. 2013;31(11):1415–21.
 45. Kruser TJ, Armstrong EA, Ghia AJ, Huang S, Wheeler DL, Radinsky R, et al. Augmentation of Radiation Response by Panitumumab in Models of Upper Aerodigestive Tract Cancer. *Int J Radiat Oncol Biol Phys*. 2008;72(2):534–42.
 46. Schneider-Merck T, Lammerts van Bueren JJ, Berger S, Rossen K, van Berkel PHC, Derer S, et al. Human IgG2 antibodies against epidermal growth factor receptor effectively trigger antibody-dependent cellular cytotoxicity but, in contrast to IgG1, only by cells of myeloid lineage. *J Immunol*. 2010;184(1):512–20.
 47. Boeckx C, Op de Beeck K, Wouters A, Deschoolmeester V, Limame R, Zwaenepoel K, et al. Overcoming cetuximab resistance in HNSCC: The role of AURKB and DUSP proteins. *Cancer Lett*. 2014;354(2):365–77.
 48. Stabile LP, Egloff AM, Gibson MK, Gooding WE, Ohr J, Zhou P, et al. IL6 is associated with response to dasatinib and cetuximab: Phase II clinical trial with mechanistic correlates in cetuximab-resistant head and neck cancer. *Oral Oncol*. 2017;69:38–45.
 49. Licitra L, Mesia R, Rivera F, Remenar E, Hitt R, Erfan J, et al. Evaluation of EGFR gene copy number as a predictive biomarker for the efficacy of cetuximab in combination with chemotherapy in the first-line treatment of recurrent and/or metastatic squamous cell

- carcinoma of the head and neck: EXTREME study. *Ann Oncol.* 2011;22(5):1078–87.
50. Licitra L, Sto S, Kerr KM, Cutsem E Van, Pirker R, Hirsch FR, et al. Predictive value of epidermal growth factor receptor expression for first-line chemotherapy plus cetuximab in patients with head and neck and colorectal cancer : Analysis of data from the EXTREME and CRYSTAL studies. 2013;1161–8.
51. Loupakis F, Ruzzo A, Cremolini C, Vincenzi B, Salvatore L, Santini D, et al. KRAS codon 61, 146 and BRAF mutations predict resistance to cetuximab plus irinotecan in KRAS codon 12 and 13 wild-type metastatic colorectal cancer. *Br J Cancer.* 2009;101(4):715–21.
52. Rampias T, Giagini A, Siolos S, Matsuzaki H, Sasaki C, Scorilas A, et al. RAS/PI3K crosstalk and cetuximab resistance in head and neck squamous cell carcinoma. *Clin Cancer Res.* 2014;20(11):2933–46.
53. Braig F, Voigtländer M, Schieferdecker A, Busch C-J, Laban S, Grob T, et al. Liquid biopsy monitoring uncovers acquired RAS-mediated resistance to cetuximab in a substantial proportion of patients with head and neck squamous cell carcinoma. *Oncotarget.* 2015;7(28).
54. Yonesaka K, Zejnullahu K, Okamoto I, Satoh T, Cappuzzo F, Souglakos J, et al. Activation of ERBB2 Signaling Causes Resistance to the EGFR-Directed Therapeutic Antibody Cetuximab. *Sci Transl Med.* 2011;3(99):99ra86.
55. Wang D, Qian G, Zhang H, Magliocca KR, Nannapaneni S, Amin ARM, et al. HER3 Targeting Sensitizes HNSCC to Cetuximab by Reducing HER3 Activity and HER2 / HER3 Dimerization : Evidence from Cell Line and Patient-Derived Xenograft Models. 2016;4:1–11.

56. Leonard B, Brand TM, O’Keefe RA, Lee ED, Zeng Y, Kemmer JD, et al. BET inhibition overcomes receptor tyrosine kinase-mediated cetuximab resistance in HNSCC. *Cancer Res.* 2018;78(15):4331–3.
57. Stuhlmiller TJ, Miller SM, Zawistowski JS, Nakamura K, Beltran AS, Duncan JS, et al. Inhibition of Lapatinib-Induced Kinome Reprogramming in ERBB2-Positive Breast Cancer by Targeting BET Family Bromodomains Article Inhibition of Lapatinib-Induced Kinome Reprogramming in ERBB2-Positive Breast Cancer by Targeting BET Family Bromodomains. *Cell Rep.* 2015;11(3):390–404.
58. Stratikopoulos EE, Dendy M, Szabolcs M, Khaykin AJ, Lefebvre C, Zhou M-M, et al. Kinase and BET Inhibitors Together Clamp Inhibition of PI3K Signaling and Overcome Resistance to Article Kinase and BET Inhibitors Together Clamp Inhibition of PI3K Signaling and Overcome Resistance to Therapy. *Cancer Cell.* 2015;27(6):837–51.
59. Filippakopoulos P, Qi J, Picaud S, Shen Y, Smith WB, Fedorov O, et al. Selective inhibition of BET bromodomains. *Nature.* 2010;468(7327):1067–73.
60. Wang Z, Martin D, Molinolo A a, Patel V, Iglesias-Bartolome R, Sol Degese M, et al. mTOR co-targeting in cetuximab resistance in head and neck cancers harboring PIK3CA and RAS mutations. *J Natl Cancer Inst.* 2014;106(9):1–11.
61. Sen M, Joyce S, Panahandeh M, Li C, Thomas SM, Maxwell J, et al. Targeting Stat3 abrogates EGFR inhibitor resistance in cancer. *Clin Cancer Res.* 2012;18(18):4986–96.
62. Bonner JA, Yang ES, Trummell HQ, Newsheem S, Willey CD, Raisch KP. Inhibition of STAT-3 results in greater cetuximab sensitivity in head and neck squamous cell carcinoma. *Radiother Oncol.* 2011;99(3):339–43.
63. Kishimoto T. IL-6: From its discovery to clinical applications. *Int Immunol.*

- 2010;22(5):347–52.
64. Yu H, Lee H, Herrmann A, Buettner R, Jove R. Revisiting STAT3 signalling in cancer: new and unexpected biological functions. *Nat Rev Cancer*. 2014;14(11):736–46.
 65. Johnson DE, O’Keefe RA, Grandis JR. Targeting the IL-6/JAK/STAT3 signalling axis in cancer. *Nat Rev Clin Oncol*. 2018;15(4):234–48.
 66. Ernst M, Jenkins BJ. Acquiring signalling specificity from the cytokine receptor gp130. *Trends Genet*. 2004;20(1):23–32.
 67. Wolf J, Rose-john S, Garbers C. Interleukin-6 and its receptors: A highly regulated and dynamic system. *Cytokine*. 2014;70(1):11–20.
 68. Rose-John S, Elson G, Jones SA. Interleukin-6 biology is coordinated by membrane-bound and soluble receptors : role in inflammation and cancer. 2006;80(August):227–36.
 69. Haan C, Heinrich PC, Behrmann I. Structural requirements of the interleukin-6 signal transducer gp130 for its interaction with Janus kinase 1: the receptor is crucial for kinase activation. *Biochem J*. 2002;361:105–11.
 70. Fletcher EVM, Love-Homan L, Sobhakumari A, Feddersen CR, Koch AT, Goel A, et al. EGFR inhibition induces proinflammatory cytokines via NOX4 in HNSCC. *Mol Cancer Res*. 2013;11(12):1574–84.
 71. Berkant Avcı A, Feist E, Rüdiger Burmester G. Targeting IL-6 or IL-6 receptor in rheumatoid arthritis: What’s the difference? *BioDrugs*. 2018;32(6):531–46.
 72. Le RQ, Li L, Yuan W, Short SS, Nie L, Habtemariam BA, et al. FDA approval summary: Tocilizumab for treatment of chimeric antigen receptor T cell-induced severe or life-threatening cytokine release syndrome. *Oncologist*. 2018;23:943–7.
 73. Tanaka T, Kishimoto T. The biology and medical implications of interleukin-6. *Cancer*

- Immunol Res. 2014;2(4):288–94.
74. Kurzrock R, Voorhees PM, Casper C, Furman RR, Fayad L, Lonial S, et al. A phase I, open-label study of siltuximab, an anti-IL-6 monoclonal antibody, in patients with B-cell non-hodgkin lymphoma, multiple myeloma, or castleman disease. *Clin Cancer Res.* 2013;19(13):3659–70.
 75. Fleischmann R, Kremer J, Cush J, Schulze-Koops H, Connell CA, Bradley JD, et al. Placebo-controlled trial of tofacitinib monotherapy in rheumatoid arthritis. *New Engl Jounal Med.* 2012;367(6):495–507.
 76. Harrison CN, Vannucchi AM, Kiladjian J-J, Al-ali HK, Gisslinger H, Knoops L, et al. Long-term findings from COMFORT-II, a phase 3 study of ruxolitinib vs best available therapy for myelo fi brosis. *Leukemia.* 2016;30(May):1701–7.
 77. Hong D, Kurzrock R, Kim Y, Woessner R, Younes A, Nemunaitis J, et al. AZD9150, a next-generation antisense oligonucleotide inhibitor of STAT3 with early evidence of clinical activity in lymphoma and lung cancer. *Sci Transl Med.* 2015;7(314):314ra185.
 78. Sen M, Thomas SM, Kim S, Yeh JI, Ferris RL, Johnson JT, et al. First-in-human trial of a STAT3 decoy oligonucleotide in head and neck tumors: Implications for cancer therapy. *Cancer Discov.* 2012;2(8):694–705.
 79. Gasparian A V, Burkhart C a, Purnal A a, Brodsky L, Pal M, Saranadasa M, et al. Curaxins: Anticancer compounds that simultaneously suppress NF- κ B and activate p53 by targeting FACT. *Sci Transl Med.* 2011;3(95):95ra74.
 80. De S, Lindner DJ, Coleman CJ, Wildey G, Dowlati A, Stark GR. The FACT inhibitor CBL0137 synergizes with cisplatin in small-cell lung cancer by increasing NOTCH1 expression and targeting tumor-initiating cells. 2018;78(12):2396–407.

81. Stanam A, Love-Homan L, Joseph TS, Espinosa-Cotton M, Simons AL. Upregulated interleukin-6 expression contributes to erlotinib resistance in head and neck squamous cell carcinoma. *Mol Oncol*. 2015;
82. Johnston PA, Grandis JR. STAT3 signaling: anticancer strategies and challenges. *Mol Interv*. 2011;11(1):18–26.
83. Sriuranpong V, Park JI, Amornphimoltham P, Patel V, Nelkin BD. Epidermal growth factor receptor-independent constitutive activation of STAT3 in head and neck squamous cell carcinoma is mediated by the autocrine/paracrine stimulation of the interleukin 6/gp130 cytokine system. *Cancer Res*. 2003;63:2948–56.
84. Mihara M, Hashizume M, Yoshida H, Suzuki M, Shiina M. IL-6/IL-6 receptor system and its role in physiological and pathological conditions. *Clin Sci*. 2011;122(4):143–59.
85. Sun Kim H, Chen Y-C, Nör F, Warner KA, Andrews A, Wagner VP, et al. Endothelial-derived interleukin-6 induces cancer stem cell motility by generating a chemotactic gradient towards blood vessels. *Oncotarget*. 2017;8(59):100339–52.
86. Blakely CM, Pazarentzos E, Olivas V, Asthana S, Yan JJ, Tan I, et al. NF- κ B-Activating Complex Engaged in Response to EGFR Oncogene Inhibition Drives Tumor Cell Survival and Residual Disease in Lung Cancer. *Cell Rep*. 2015;11(1):98–110.
87. Gao J, Zhao S, Halstensen TS. Increased interleukin-6 expression is associated with poor prognosis and acquired cisplatin resistance in head and neck squamous cell carcinoma. *Oncol Rep*. 2016;35:3265–74.
88. Verboogen RJ, Revelo NH, Beest M, Bogaart G Van Den. Interleukin- 6 secretion is limited by self-signaling in endosomes. 2019;11:144–57.
89. Fisher DT, Appenheimer MM, Evans SS. The two faces of IL-6 in the tumor

- microenvironment. *Semin Immunol.* 2014 Feb;26(1):38–47.
90. Yu H, Pardoll D, Jove R. STATs in cancer inflammation and immunity: a leading role for STAT3. *Nat Rev Cancer.* 2009;9(11):798–809.
 91. Kline CN, Joseph NM, Grenert JP, Van Ziffle J, Talevich E, Onodera C, et al. Targeted next-generation sequencing of pediatric neuro-oncology patients improves diagnosis, identifies pathogenic germline mutations, and directs targeted therapy. *Neuro Oncol.* 2017;19(5):699–709.
 92. Lv D, Jia F, Hou Y, Sang Y, Alvarez AA, Zhang W, et al. Histone Acetyltransferase KAT6A Upregulates PI3K / AKT Signaling through TRIM24 Binding. 2017;77(22).
 93. Kennedy J, Goudie D, Blair E, Chandler K, Joss S, McKay V, et al. KAT6A Syndrome: Genotype – phenotype correlation in 76 patients with pathogenic KAT6A variants. *Genet Med.* 2019;21(4):850–60.
 94. Pan C, Izreig S, Yarbrough WG, Issaeva N. NSD1 mutations by HPV status in head and neck cancer : differences in survival and response to DNA-damaging agents. *Cancers Head Neck.* 2019;4(3):1–13.
 95. Stein-O'Brien G, Kagohara LT, Li S, Thakar M, Ranaweera R, Ozawa H, et al. Integrated time course omics analysis distinguishes immediate therapeutic response from acquired resistance. *Genome Med.* 2018;10(1):1–22.
 96. Bagchi A, Papazoglu C, Wu Y, Capurso D, Brodt M, Francis D, et al. CHD5 Is a Tumor Suppressor at Human 1p36. 2007;459–75.
 97. Cerami E, Gao J, Dogrusoz U, Gross BE, Sumer SO, Arman B, et al. The cBio Cancer Genomics Portal: An Open Platform for Exploring Multidimensional Cancer Genomics Data. 2012;(May).

98. Gao J, Aksoy BA, Dogrusoz U, Dresdner G, Gross B, Sumer SO, et al. Integrative Analysis of Complex Cancer Genomics and Clinical Profiles Using the cBioPortal Complementary Data Sources and Analysis Options. *Sci Signal*. 2013;6(269):1–20.
99. Atlas TCG. Integrated Genomic Characterization of Papillary Thyroid Carcinoma. *Cell*. 2014;159:676–90.
100. Krishnamoorthy GP, Davidson NR, Leach SD, Zhao Z, Lowe SW, Lee G, et al. EIF1AX and RAS Mutations Cooperate to Drive Thyroid Tumorigenesis through ATF4 and c-MYC. 2018;(february 2019).
101. Martin M, Masshofer L, Temming P, Rahmann S, Metz C, Bornfeld N, et al. Exome sequencing identifies recurrent somatic mutations in EIF1AX and SF3B1 in uveal melanoma with disomy 3. *Nat Genet*. 2013;45(8):933–6.
102. Cheung LWT, Hennessy BT, Li J, Yu S, Myers AP, Djordjevic B, et al. High frequency of PIK3R1 and PIK3R2 mutations in endometrial cancer elucidates a novel mechanism for regulation of PTEN protein stability. *Cancer Discov*. 2011;1(2):170–85.
103. Beck TN, Georgopoulos R, Shagisultanova EI, Sarcu D, Handorf EA, Dubyk C, et al. EGFR and RB1 as Dual Biomarkers in HPV-Negative Head and Neck Cancer. *Mol Cancer Ther*. 2016;15(10):2486–97.

Publishing Agreement

It is the policy of the University to encourage the distribution of all theses, dissertations, and manuscripts. Copies of all UCSF theses, dissertations, and manuscripts will be routed to the library via the Graduate Division. The library will make all theses, dissertations, and manuscripts accessible to the public and will preserve these to the best of their abilities, in perpetuity.

Please sign the following statement:

I hereby grant permission to the Graduate Division of the University of California, San Francisco to release copies of my thesis, dissertation, or manuscript to the Campus Library to provide access and preservation, in whole or in part, in perpetuity.

DocuSigned by:
Rachel O'Keefe 12/10/2019
5FDF7E19D896495... Author Signature Date